

An Empirical Absolute Calibration Model using Libya 4

**Dennis Helder
Nischal Mishra
Ameya Vaidya
Dave Aaron**

**CEOS/IVOS Libya 4 Workshop
Paris, France
October 4-5, 2012**

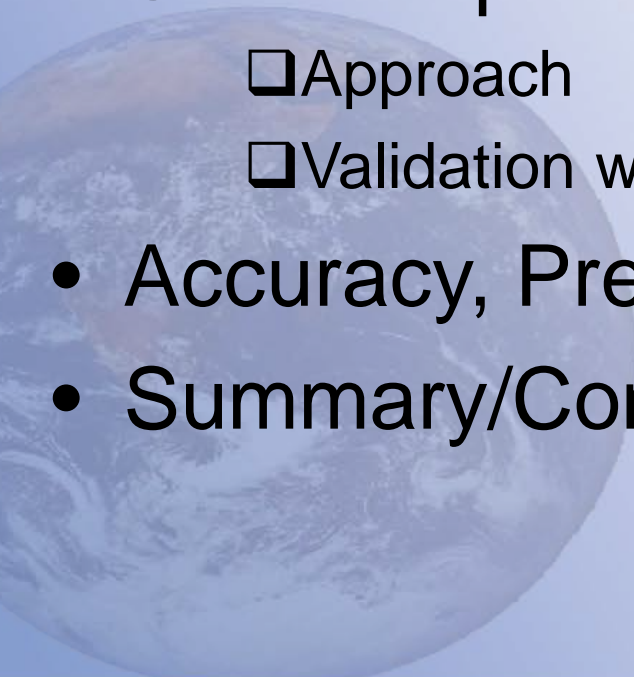


South Dakota State University
Image Processing Lab

Objective

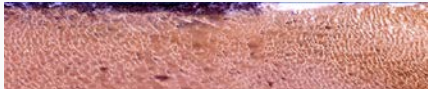
- Pseudo Invariant Calibration Sites (PICS) have been used for many years to determine the stability of optical satellite sensors.
- However, the potential exists to use PICS for **absolute** calibration of optical satellite sensors. As a sensor views a calibration panel in the laboratory during pre-launch testing, in an analogous manner consider the sensor viewing PICS while on orbit.
- Specific goals:
 - Develop a comprehensive and accurate PICS absolute calibration model that can be SI traceable.
 - Empirical approach (presented here)
 - Developing surface and atmospheric models based on satellite and meteorological observations.
 - First Principles approach (later)
 - Develop surface and atmospheric models based on the inherent physics of the site.

Outline

- Region of Interest (ROI)
 - Empirical Model
 - Approach
 - Validation with MODIS and Landsat observations
 - Semi-Empirical Model
 - Approach
 - Validation with MODIS & Landsat observations
 - Accuracy, Precision, and SI Traceability
 - Summary/Conclusions/Future Directions
- 

ROI Selection: PICS Min-Noise Algorithm

- The algorithm is based on identifying the most temporal invariant region in a WRS image using Landsat 5 lifetime trending data.
- The algorithm has been applied to most of the PICS in the Saharan region to find the optimal ROI.
- The approach involves
 - ❑ Dividing image is divided into grids of various size such as 10 by 10, 50 by 50, 100 by 100 pixel grids and the whole WRS (185x185 km) image.
 - ❑ Top regions are then identified by ranking the grids in terms of lower temporal uncertainty (standard deviation divided by mean).
 - ❑ Comparing the uncertainty of smaller portions of a site (for example, a region consisting of the top 10 ROIs or top 50 ROIs) with the uncertainty of the site as a whole can give an idea of whether it would be beneficial to use a smaller region of the site for calibration work rather than the whole site. Levene test is used for the equality of variance



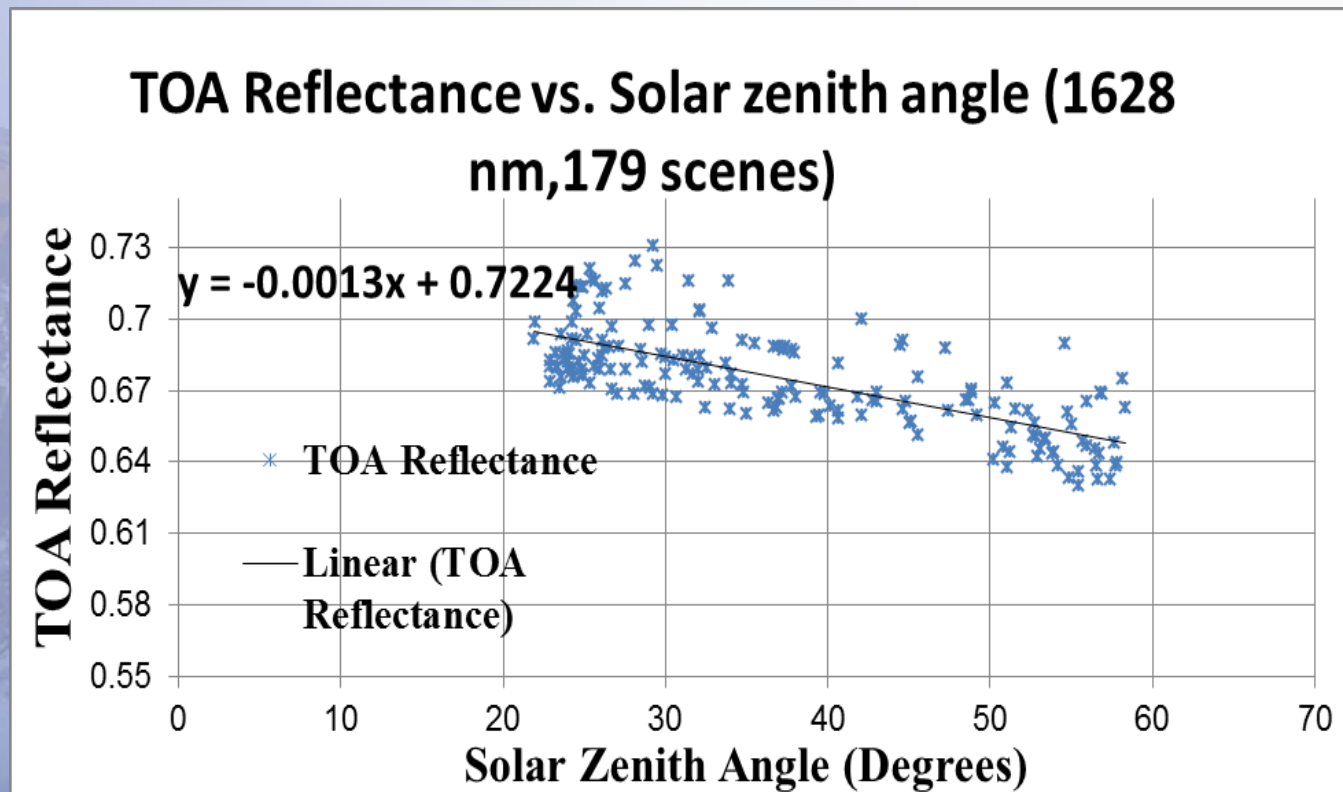
PICS List	Latitude/Longitude in Degrees								Size (km)
	Upper left (northwest)		Upper right (northeast)		Lower left (southwest)		Lower right (southeast)		
Libya 4, desert	29.754	23.127	29.482	24.862	28.249	22.751	27.991	24.481	171 × 171
Libya 1, desert	25.430	12.773	25.212	14.484	23.921	12.417	23.656	14.090	171 × 171
Arabia 2, Middle East	21.120	50.397	20.870	51.997	19.615	50.076	19.377	51.624	171 × 171
Egypt 2, Sahara desert	23.972	27.888	23.730	29.521	22.575	27.557	22.325	29.167	171 × 162
Algeria 3, Sahara desert	30.540	7.270	30.385	7.928	29.560	6.958	29.451	7.694	72 × 108
Egypt 1, Sahara desert	27.707	26.640	27.607	27.353	26.721	26.403	26.587	27.134	72 × 108
Mauritania 2, desert	20.887	9.984	20.804	9.235	19.926	10.173	19.830	9.468	72 × 108
Mauritania1, desert	19.675	10.157	19.513	-9.126	19.044	-10.309	18.891	-9.271	108 × 72
Sonoran Desert, Mexico	32.065	-114.517	31.950	-113.75	31.794	-114.585	31.680	-113.831	72 × 30
Dunhuang, China	40.269	93.919	40.220	94.288	39.736	93.758	39.687	94.112	30 × 60
Simpson Desert, Australia	-23.793	136.954	-23.942	137.951	-24.509	136.797	-24.655	137.789	99 × 81
Barreal Blanco, Argentina	-31.855	-69.461	-31.855	-69.437	-31.876	-69.463	-31.877	-69.440	2.4 × 2.4

Statistical approach to empirical BRDF model development

- Select a Hyperion channel that is atmospherically transparent. 'Most transparent' channel tend to lie in SWIR channel
- Trend the dependent variable (TOA reflectance) as a function of illumination angle (solar zenith and solar azimuth) and viewing angle.
- Apply appropriate transformation to dependent variables if any trends were observed.
- Check for correlation between independent variables. (Ex. Solar Zenith and Solar Azimuth)
- Outlier testing was performed using Bonferroni test.
- Select the best model based on R-square and residual error and test significance of predictors in the model at 95% confidence interval.

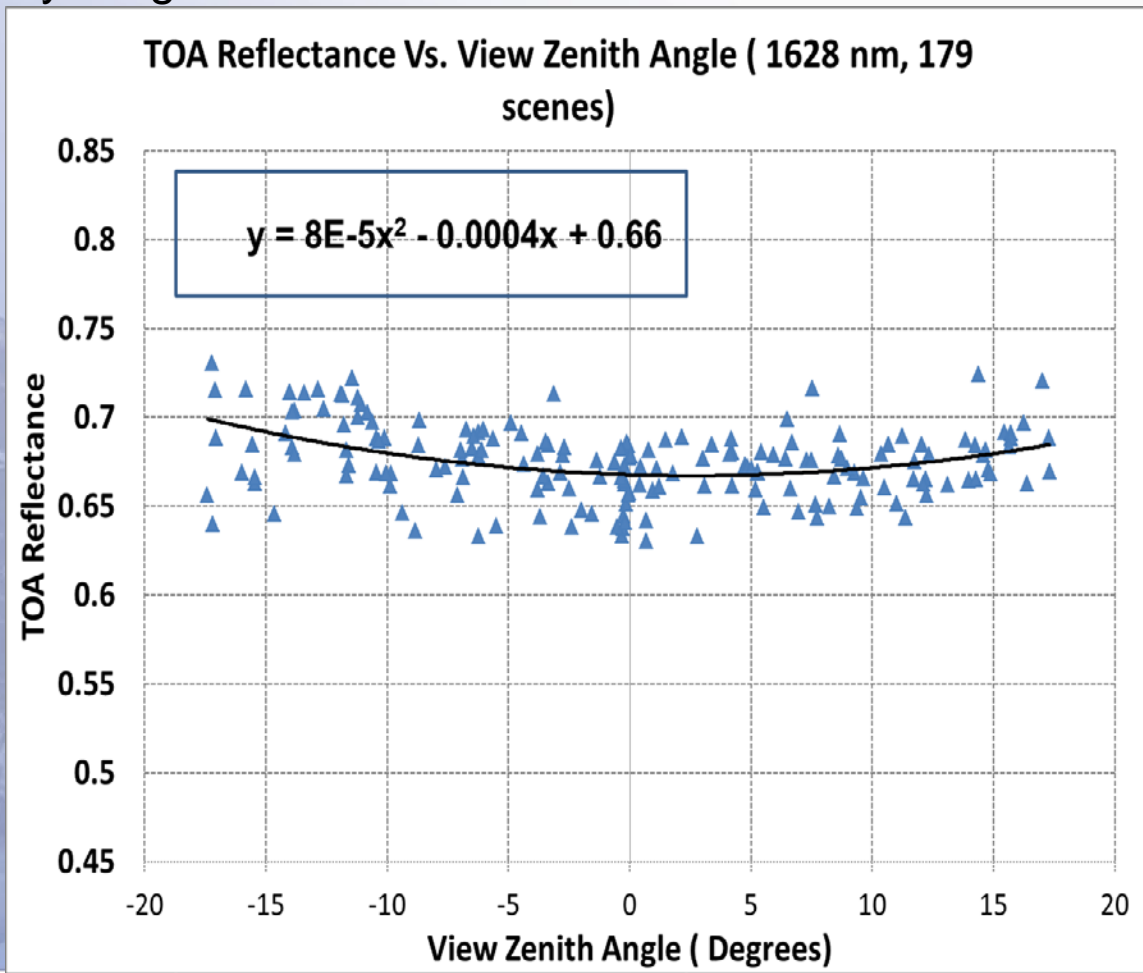
TOA Reflectance vs. Solar zenith angle

- Linear model was then used to predict the TOA reflectance as a function of zenith angle, higher order terms were statistically insignificant.
- The plot for TOA Reflectance vs. Solar zenith angle shows a negative linear trend.



TOA reflectance Vs. Viewing angle

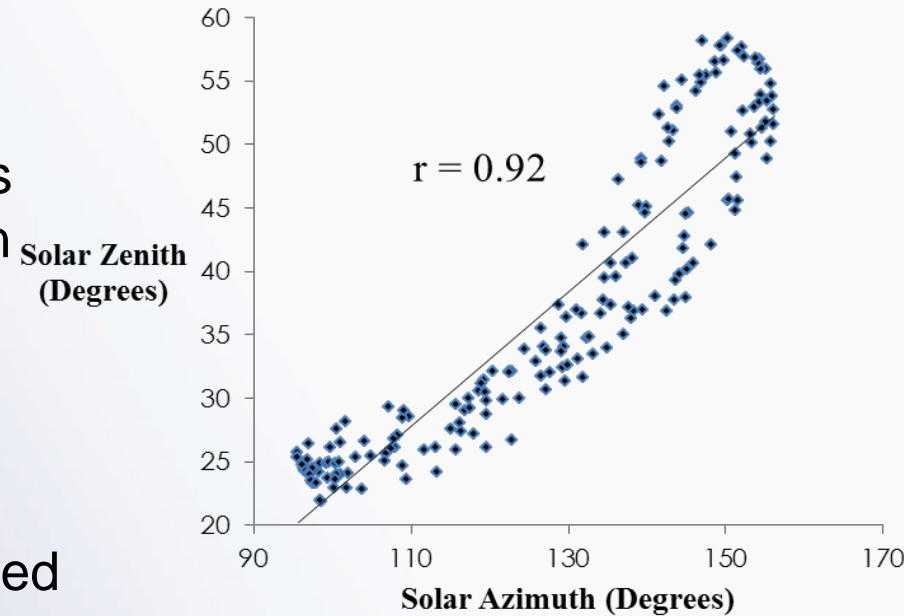
- BRDF as a function of viewing angle is clearly non-linear
- 2nd order polynomial model developed, similar to Ross-Li model; higher order terms were statistically insignificant



Correlation test and outlier rejection

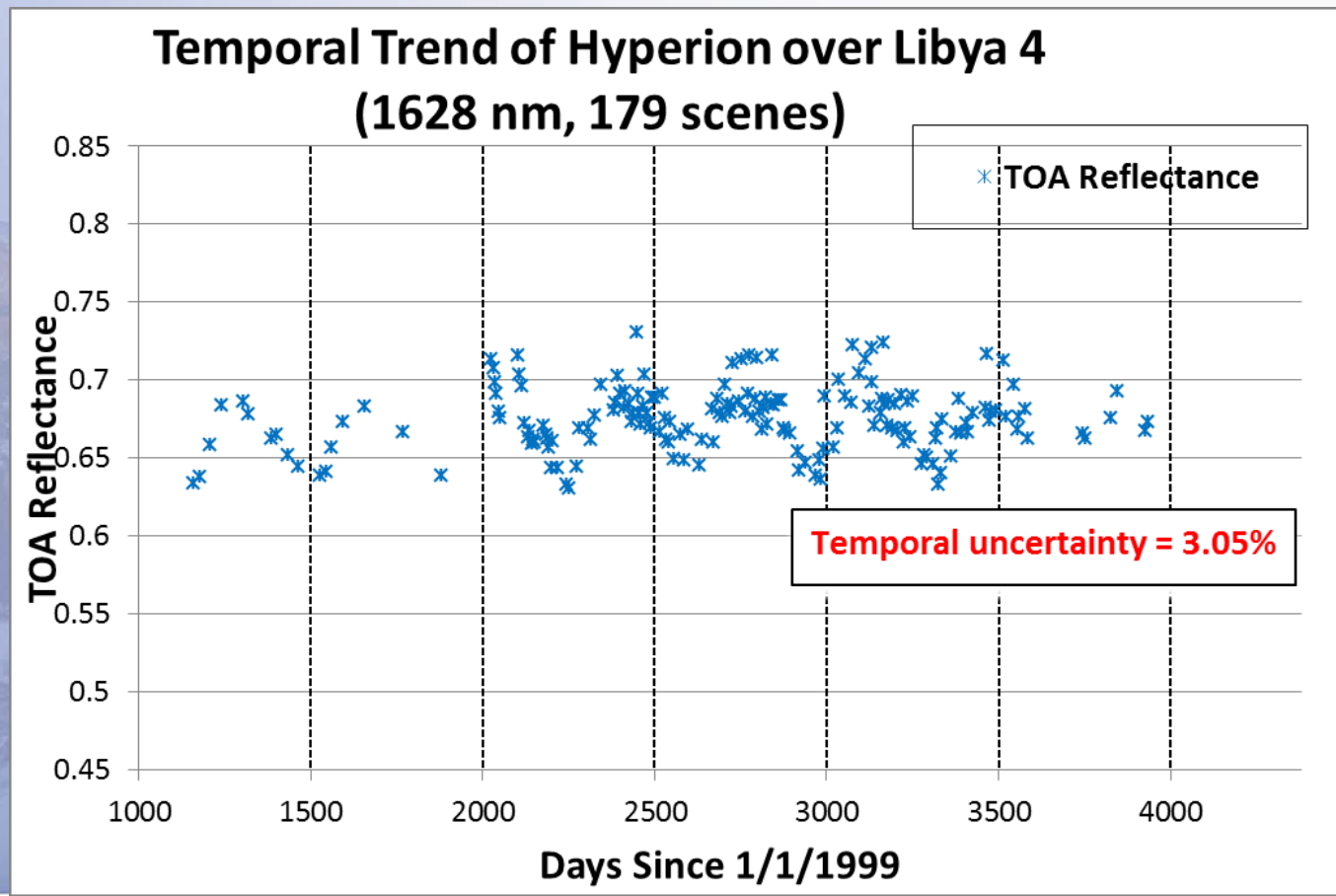
- A strong positive correlation exists between Solar Zenith and Solar Azimuth variables indicating that it is sufficient to include either variable in the model.
- Use the Bonferroni test for the 'n' observations -if the residuals are larger in magnitude than the critical value then the observation is identified as an outlier.

Correlation coefficient (r)

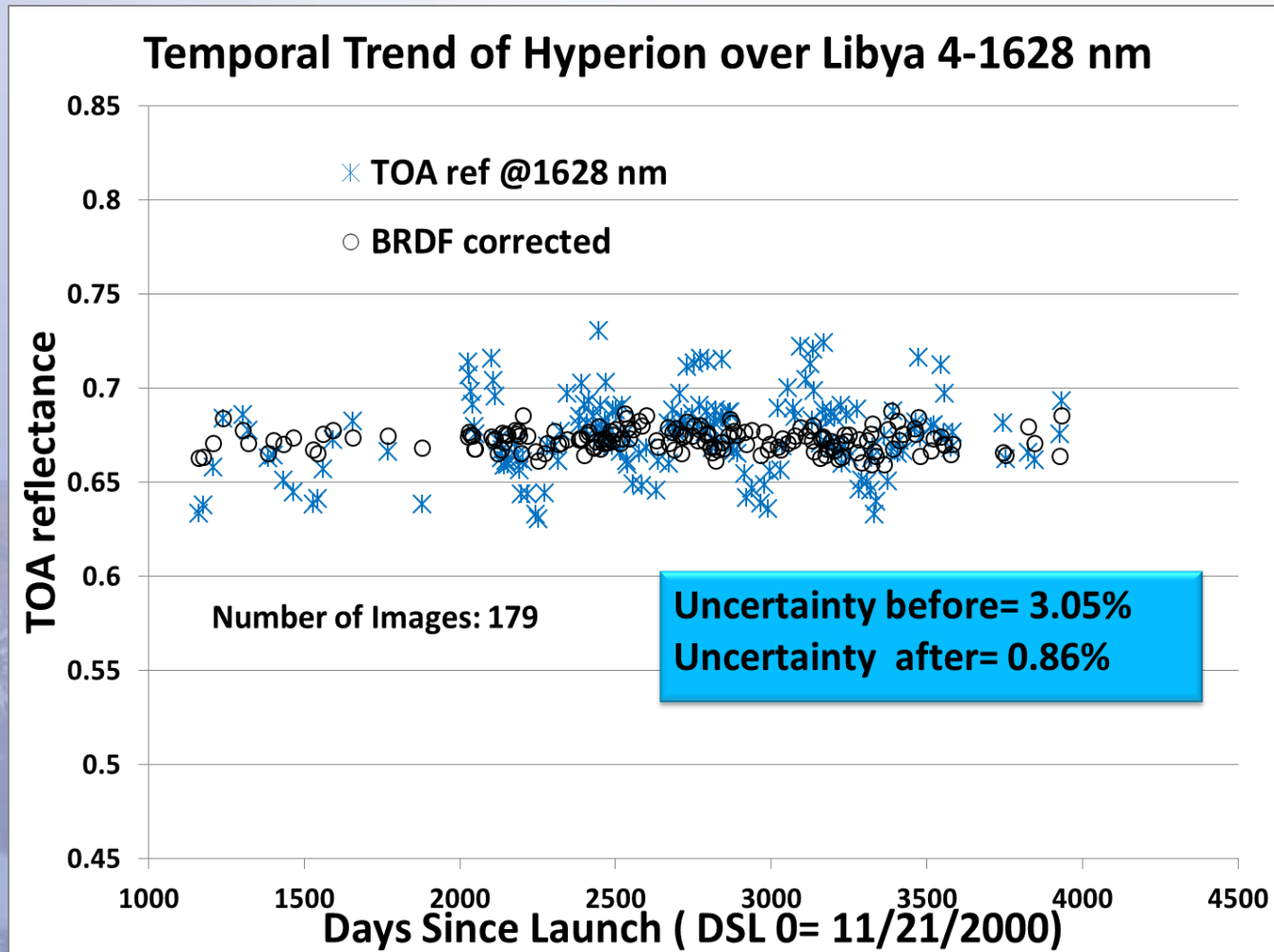


Top of atmosphere (TOA) reflectance model

- The best model was of the form $\rho(\theta_{SZ}, \theta_{VZ}, \lambda) = a_\lambda + b_\lambda * \theta_{SZ} + c_\lambda * \theta_{VZ} + d_\lambda * \theta_{VZ}^2$
- This model was applied to atmospherically cleaner channels in the SWIR and VNIR region .
- The model reduced the temporal uncertainty to better than 1%



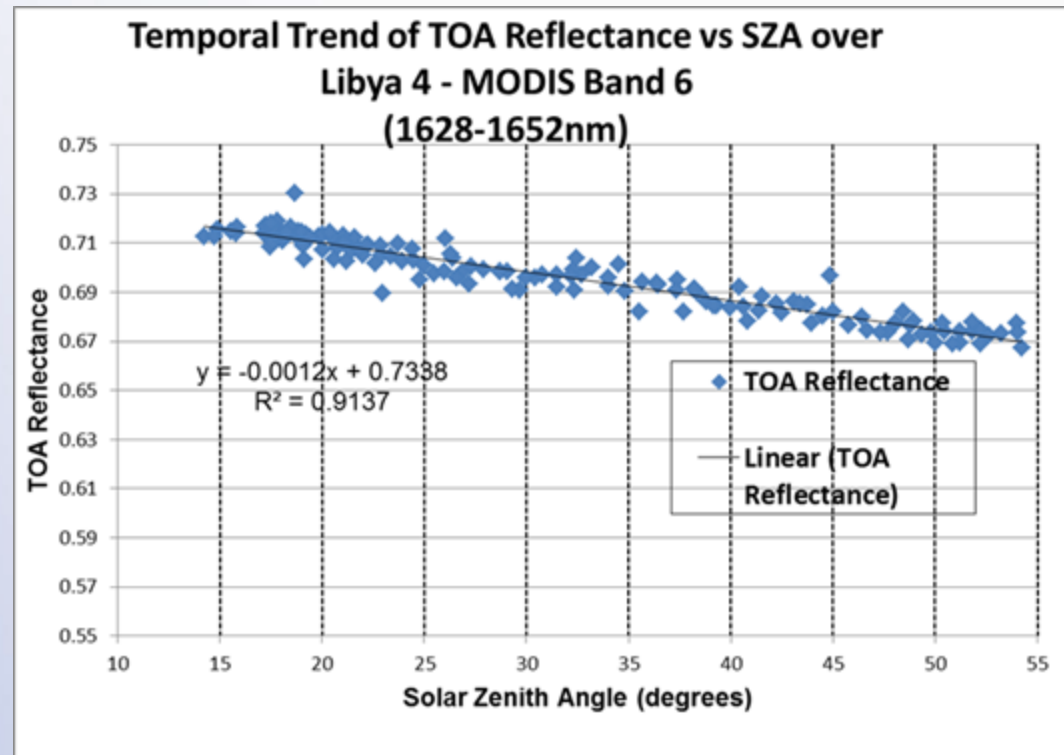
Result of the model



- Without atmospheric effects, site stability is better than 1% in atmospherically transparent channels.

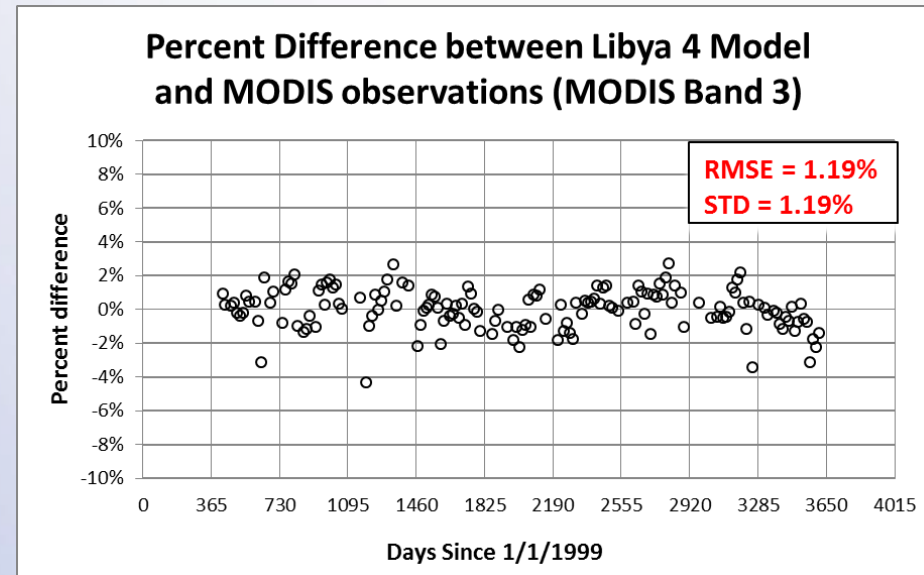
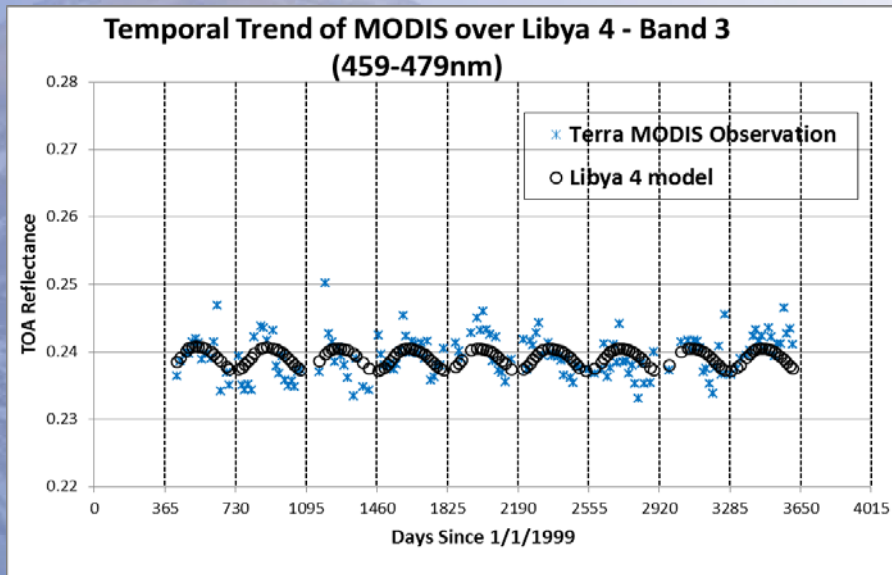
Validation of the model using Terra MODIS (nadir observations)

- The TOA reflectance model was developed for nadir looking MODIS observations.
- Example shown for SWIR 1 band shows the linear fit for solar azimuth angle.
- The modeled MODIS TOA reflectance was then compared to the actual measurements made by Terra MODIS.
- The systematic and random uncertainties were calculated for each band
- Similar procedure was developed for each channel.



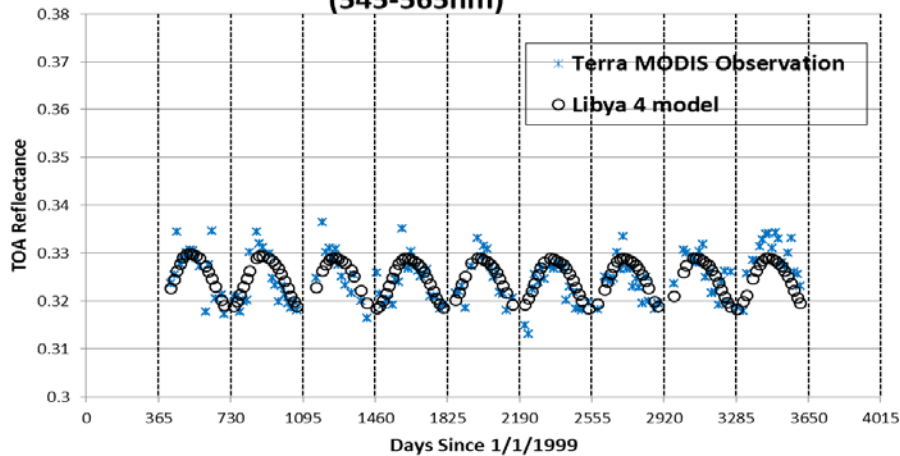
Validation of the empirical model using Terra MODIS

- For Band 1, the simple empirical model predicts the TOA reflectance to better than 1.2%
- Since visible bands are affected by aerosol scattering, there is an opportunity to bring the uncertainties further by applying corrections for scattering

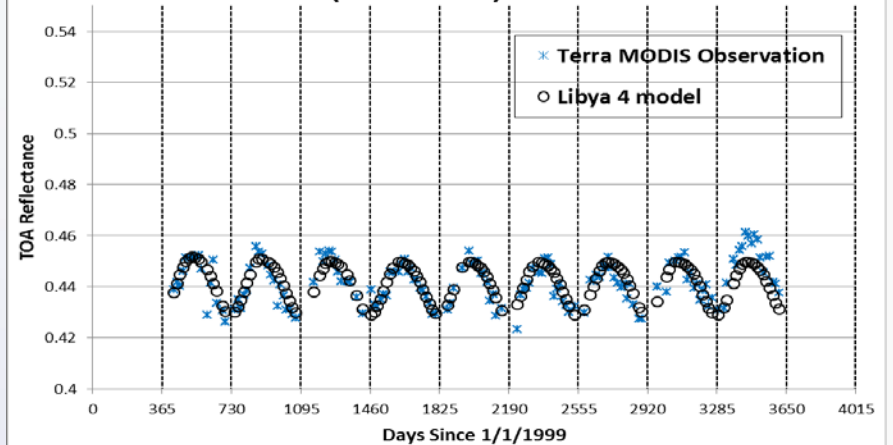


Validation results for Green and Red bands

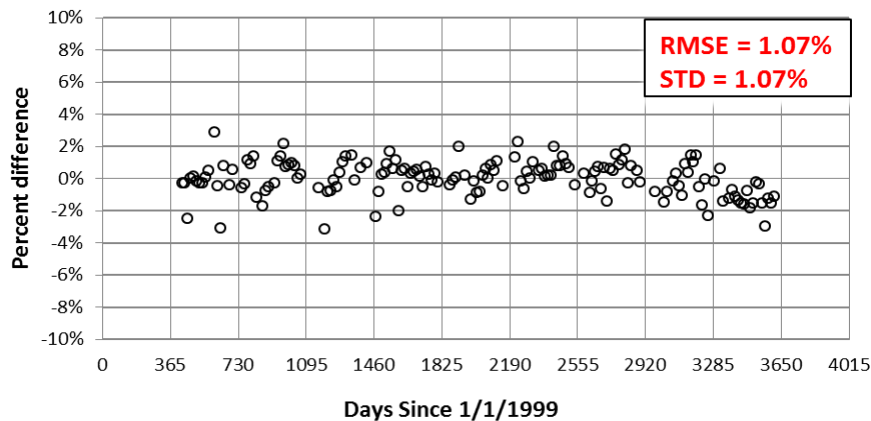
Temporal Trend of MODIS over Libya 4 - Band 4 (545-565nm)



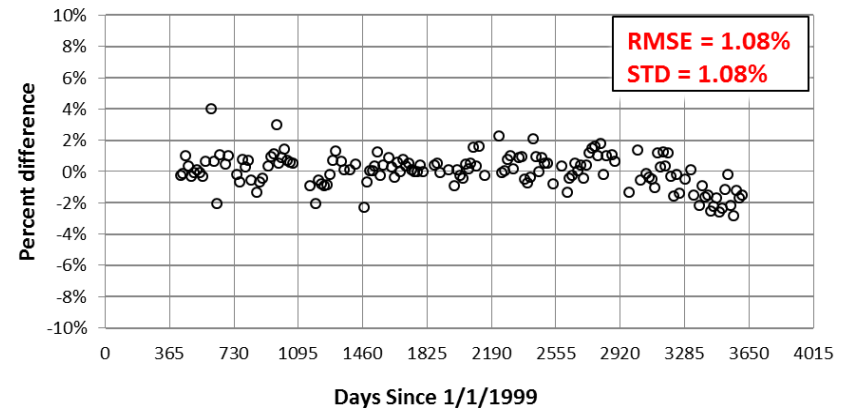
Temporal Trend of MODIS over Libya 4 - Band 1 (620-670nm)



Percent Difference between Libya 4 Model and MODIS observations (MODIS Band 4)

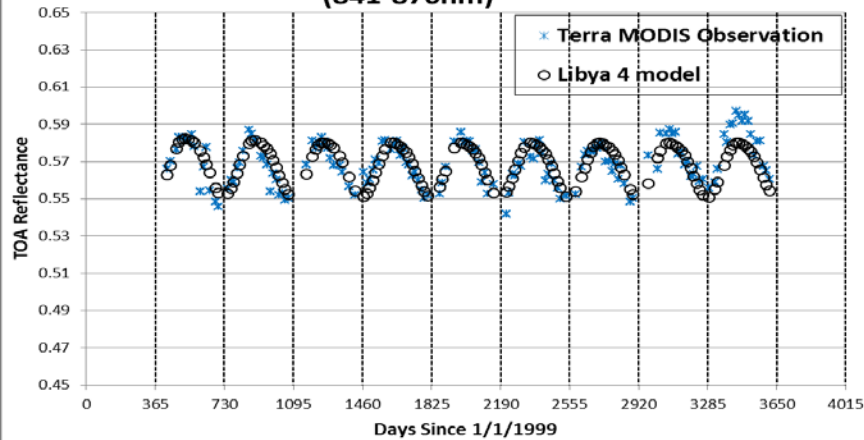


Percent Difference between Libya 4 Model and MODIS observations (MODIS Band 1)

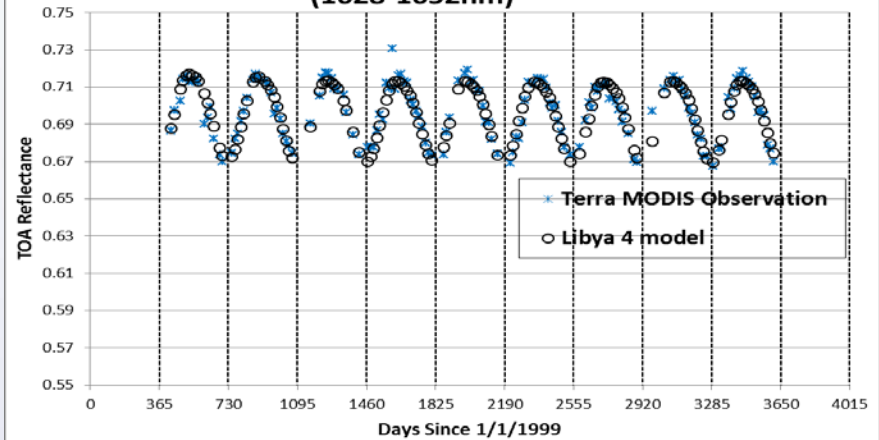


Validation results for VNIR and SWIR-1 bands

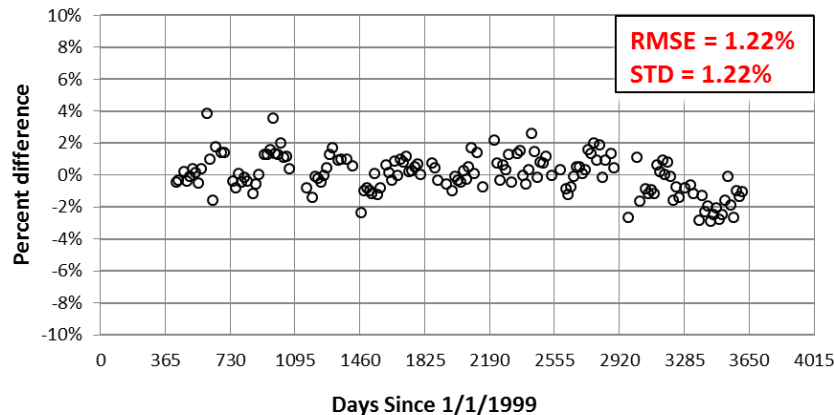
Temporal Trend of MODIS over Libya 4 - Band 2
(841-876nm)



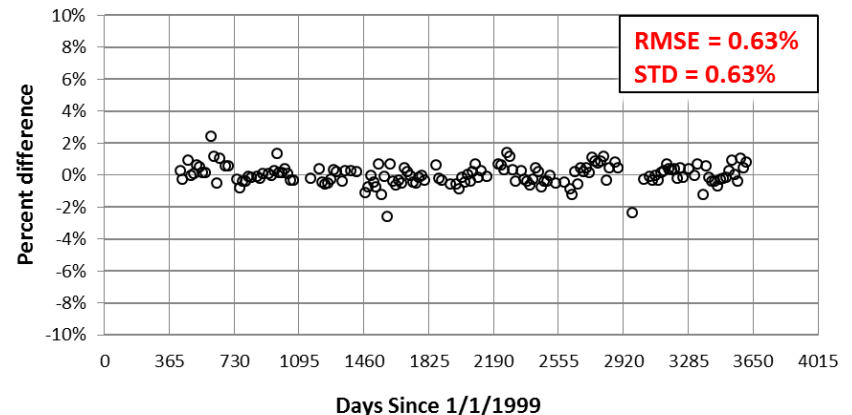
Temporal Trend of MODIS over Libya 4 - Band 6
(1628-1652nm)



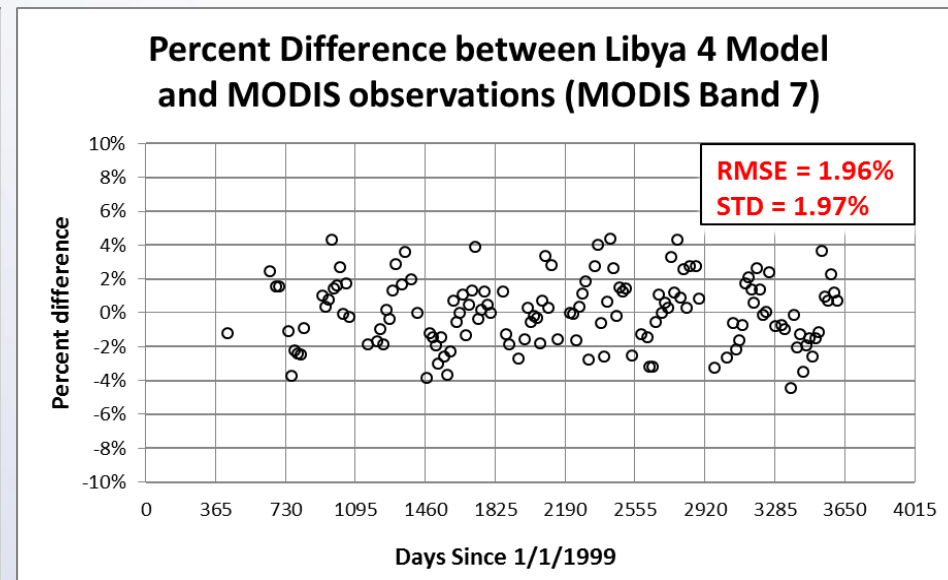
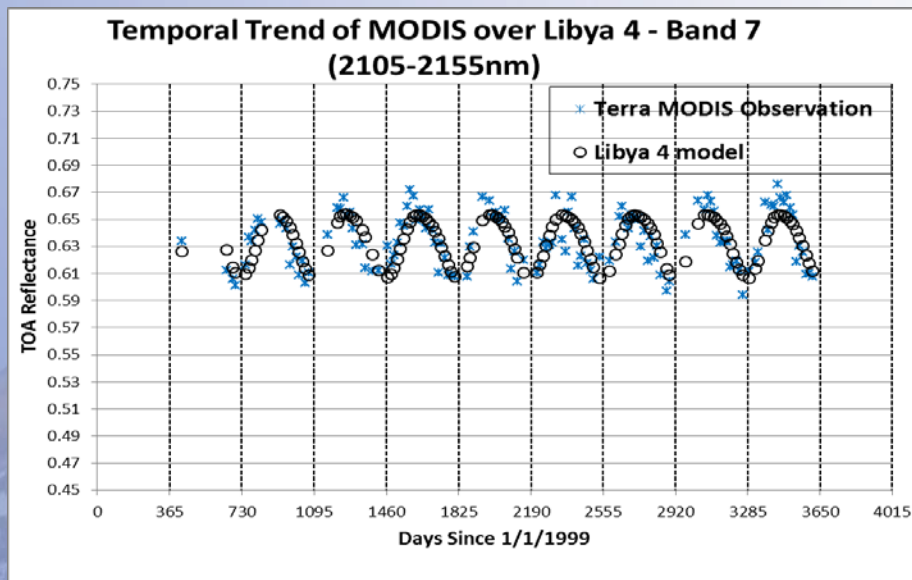
Percent Difference between Libya 4 Model and MODIS observations (MODIS Band 2)



Percent Difference between Libya 4 Model and MODIS observations (MODIS Band 6)



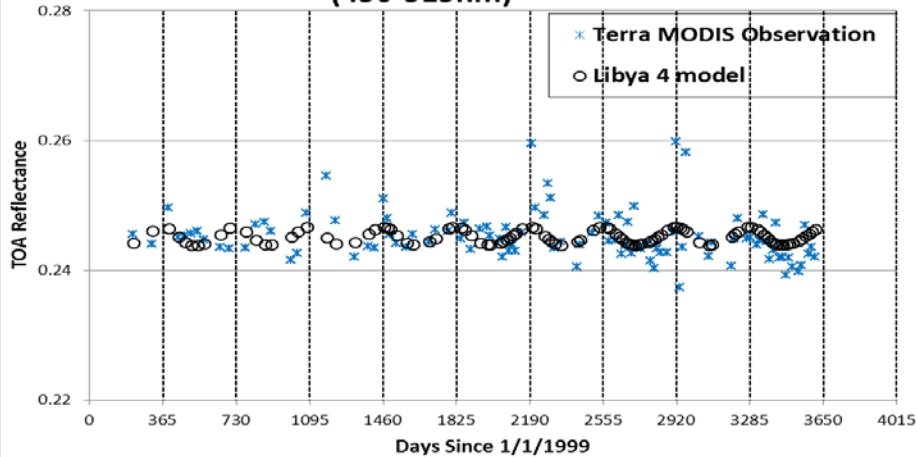
Validation results for VNIR and SWIR-2 band



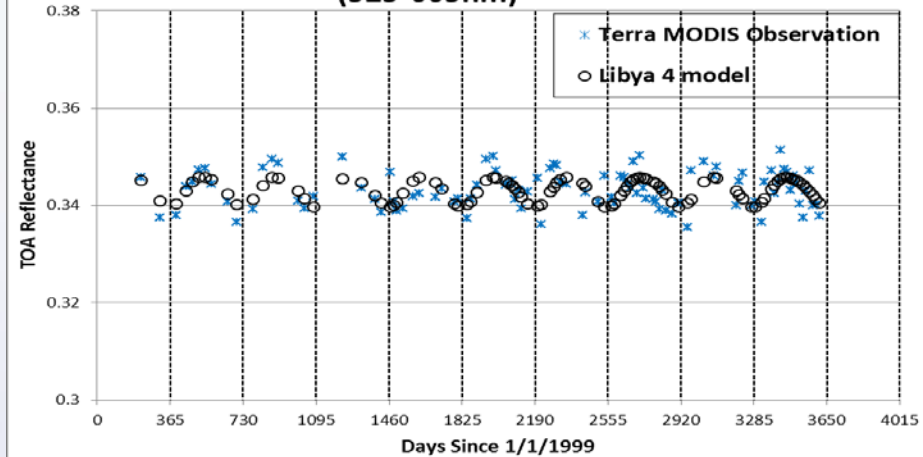
- Thus for MODIS bands, the empirical model predicts the measured TOA reflectance to better than 2%.
- Slightly higher uncertainties are seen in the SWIR band probably because of the presence of atmospheric components in this channel.

Validation of the model using Landsat 7 ETM+

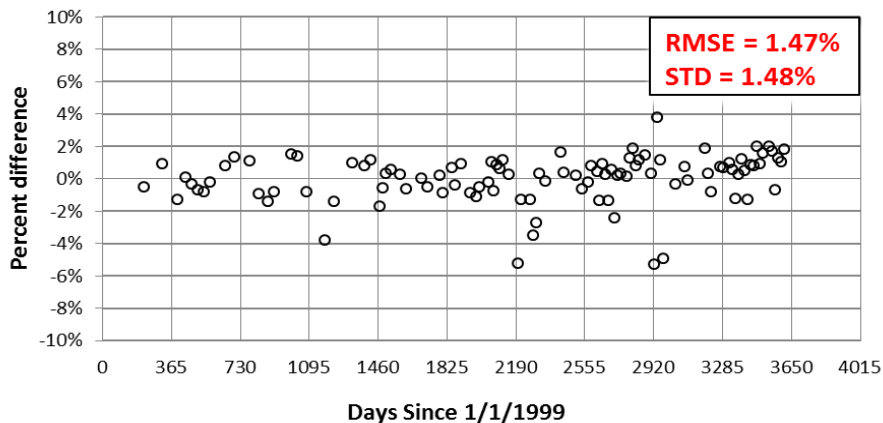
Temporal Trend of ETM+ over Libya 4 - Band 1 (450-515nm)



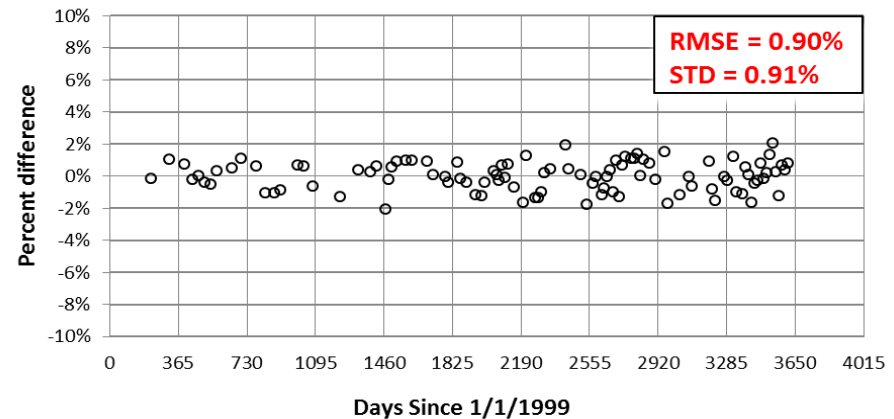
Temporal Trend of ETM+ over Libya 4 - Band 2 (525-605nm)



Percent Difference between Libya 4 Model and ETM+ observations (ETM Band 1)

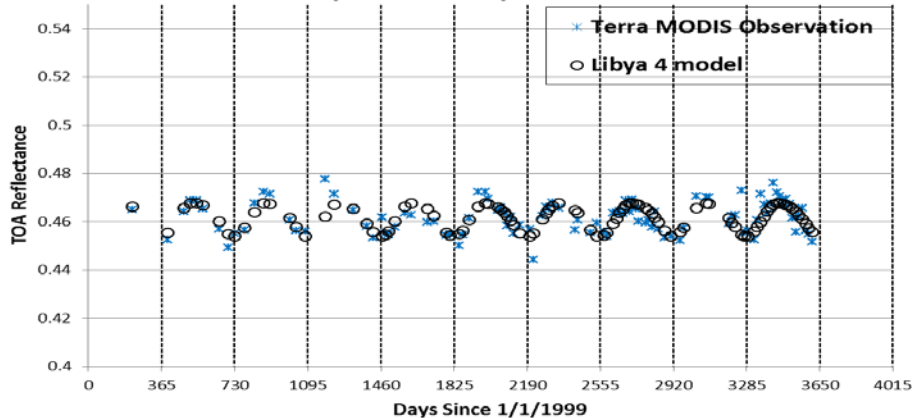


Percent Difference between Libya 4 Model and ETM+ observations (ETM Band 2)

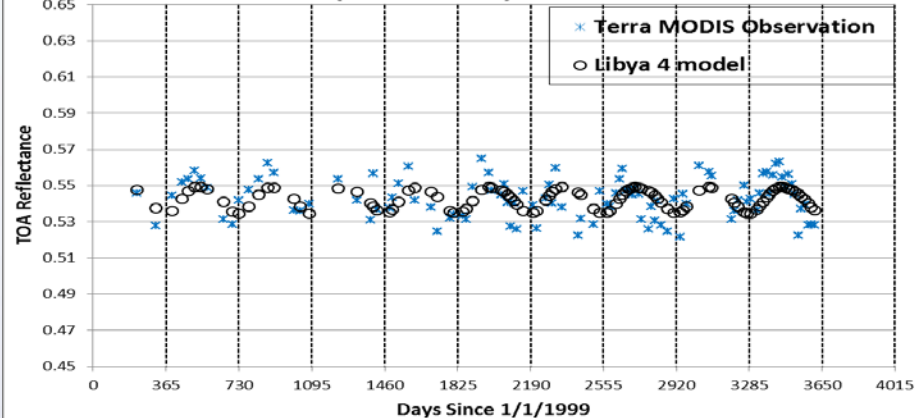


Validation of the model for red and VNIR bands

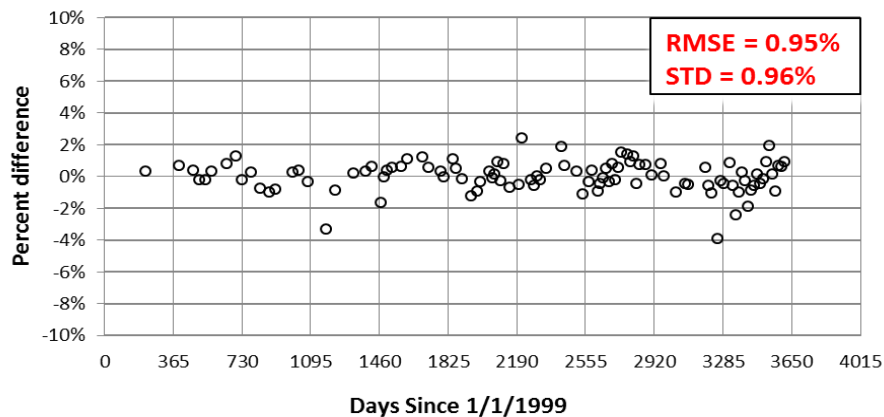
Temporal Trend of ETM+ over Libya 4 - Band 3
(630-690nm)



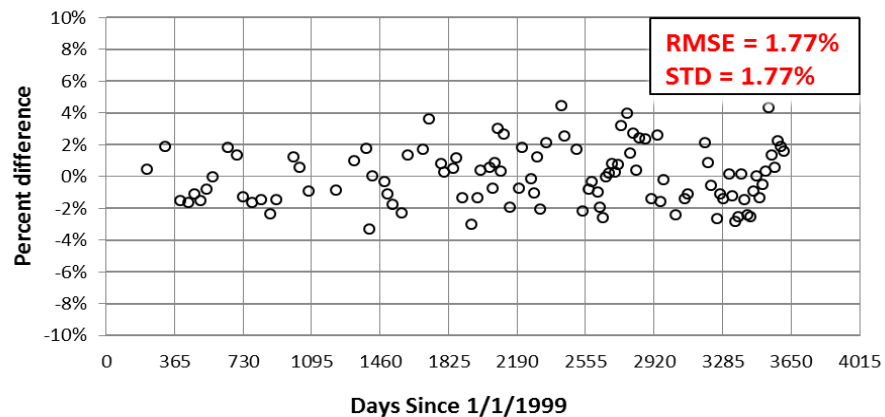
Temporal Trend of ETM+ over Libya 4 - Band 4
(750-900nm)



Percent Difference between Libya 4 Model
and ETM+ observations (ETM Band 3)

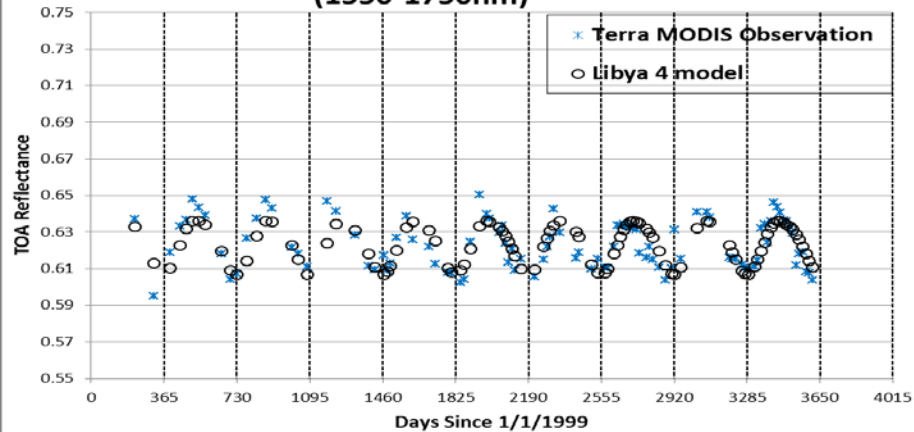


Percent Difference between Libya 4 Model
and ETM+ observations (ETM Band 4)

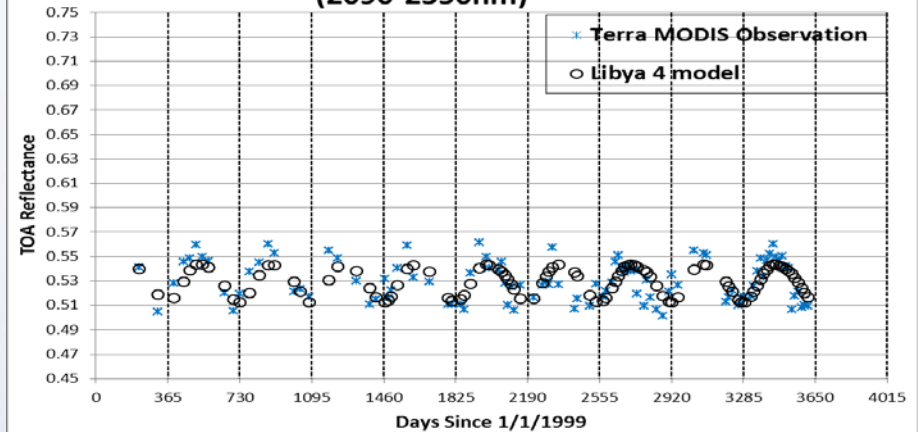


Validation of the model for SWIR-1 SWIR-2 bands

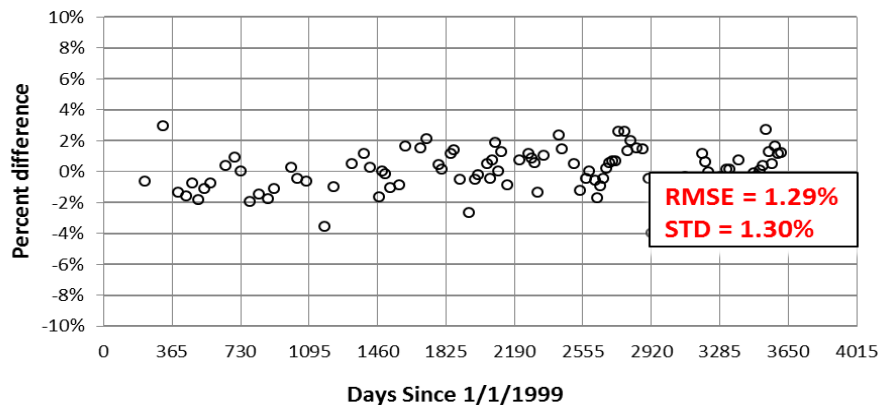
Temporal Trend of ETM+ over Libya 4 - Band 5
(1550-1750nm)



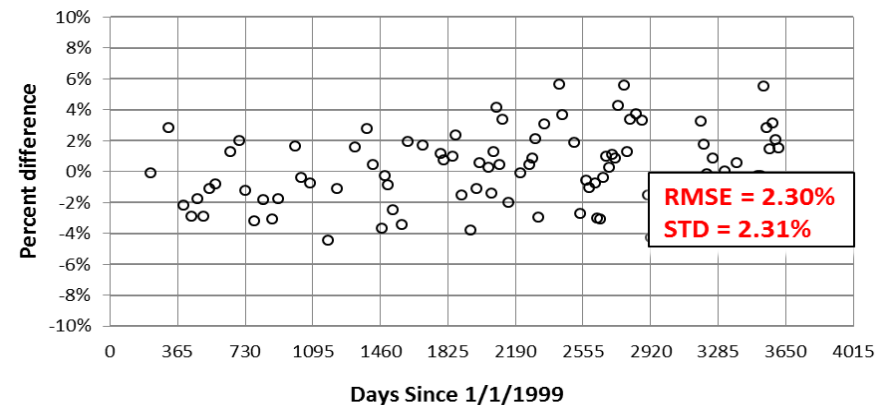
Temporal Trend of ETM+ over Libya 4 - Band 7
(2090-2350nm)



Percent Difference between Libya 4 Model
and ETM+ observations (ETM Band 5)



Percent Difference between Libya 4 Model
and ETM+ observations (ETM Band 7)



Discussion on empirical model

- The pure empirical model was based on predicting the TOA reflectance by doing the empirical fit of the TOA reflectance as a function on illumination and look angle only.
- Validation results showed that the model could predict the TOA reflectance of Landsat ETM+ and Terra MODIS to better than ~2%.
- However this “simple minded” pure empirical model is not tied to any absolute scale.
- The following section describes the development of a semi-empirical hyperspectral calibration model where a well calibrated radiometer is used as a reference for absolute calibration.

Semi-Empirical Absolute Calibration Model Approach

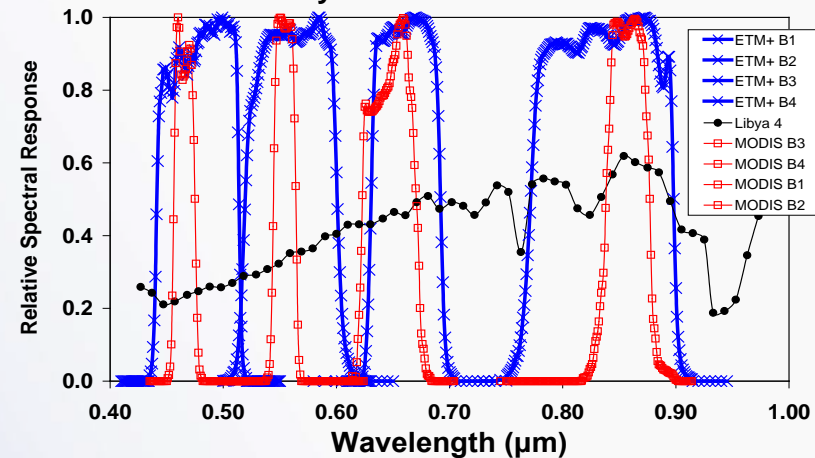
- Spectral content of the target is derived using EO-1 Hyperion
 - ❑ Terra MODIS is used as a calibrated radiometer to scale the Hyperion spectra appropriately
 - ❖ Terra has been preferred instead of AQUA because of its tandem orbit with Hyperion.
 - ❖ Diffuser based radiometric calibration of better than 3%
 - ❑ The BRDF effect due to illumination angle has been developed using Terra MODIS observations
 - ❑ The BRDF effect due to viewing angle has been developed using Hyperion observations
- The model was then validated using nadir observations from Terra MODIS and ETM+ observations

Absolute scaling factor—anchoring spectral model to Terra MODIS

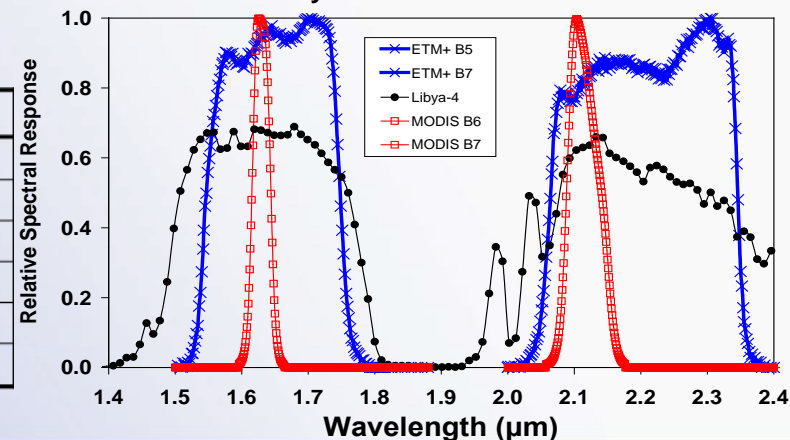
- Assuming Terra to be the calibration standard, the Hyperion spectrum can be scaled appropriately so that the model produces the same value as Terra when integrated over the Terra spectral band-pass.

- Scale factor calculated using six available same day (viewing angles $< \pm 5^\circ$, solar zenith angle of $30 \pm 5^\circ$) pairs.
- Statistical analysis indicated mean scaling values could be clustered into three groups: band 7, bands 3,2 and 6 and bands 1, 4 ($\alpha = 0.05$).
- Hyperspectral scale model was then developed using smooth linear interpolation between these three gain points.

ETM+ (Bands 1,2,3,4), MODIS (Bands 3,4,1,2) & Libya 4 TOA Reflectance



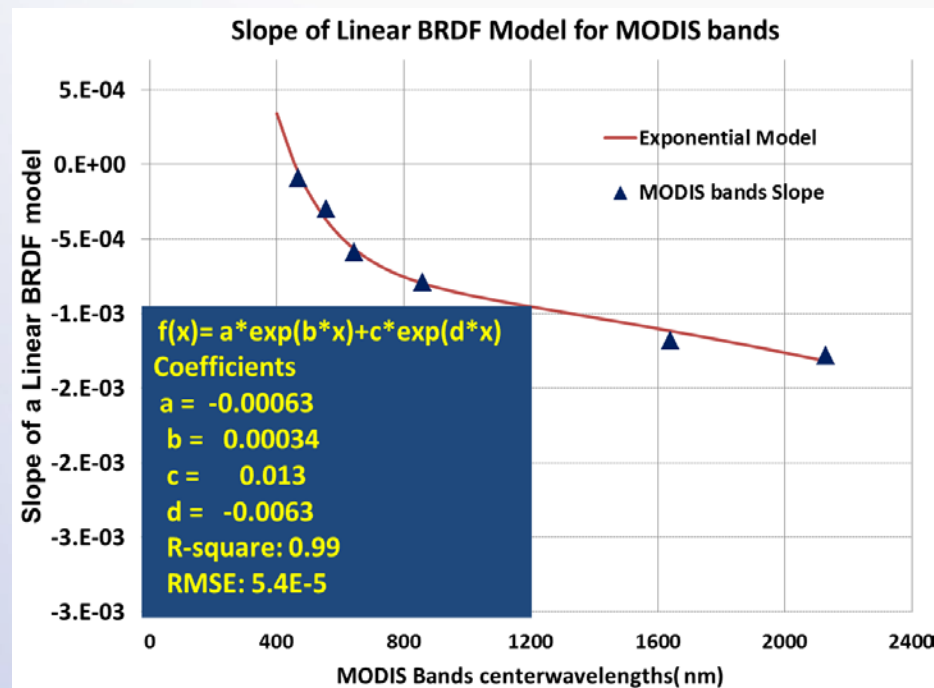
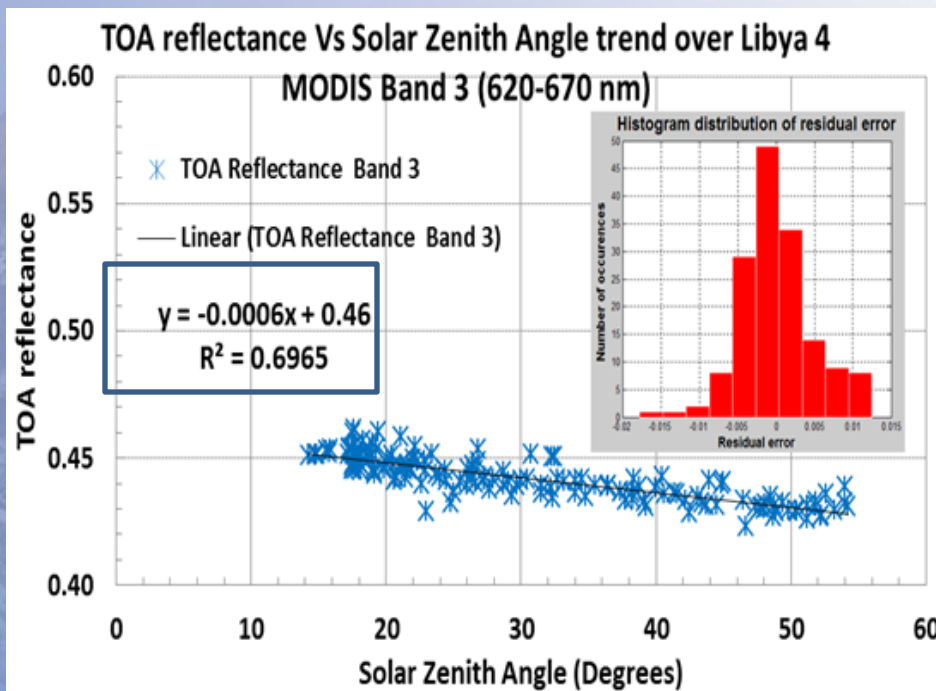
ETM+ (Bands 5,7), MODIS (Bands 6,7) & Libya 4 TOA Reflectance



MODIS Bands	7/4/2004	9/6/2004	9/22/2004	9/25/2005	6/24/2006	9/15/2007	Average	STD
3 (459-479 nm)	1.025	0.992	1.001	0.998	0.973	0.979	0.995	1.82%
4 (545-565 nm)	1.029	1.006	1.008	1.009	1.000	1.000	1.009	1.05%
1 (620-670 nm)	1.024	1.010	1.007	1.013	1.003	1.001	1.010	0.83%
2 (841-876 nm)	0.993	0.990	0.978	0.988	0.973	0.983	0.984	0.81%
6 (1628-1652 nm)	0.996	1.001	0.991	0.999	0.977	0.984	0.992	0.95%
7 (2105-2155 nm)	0.986	0.974	0.960	0.966	0.952	0.954	0.965	1.32%

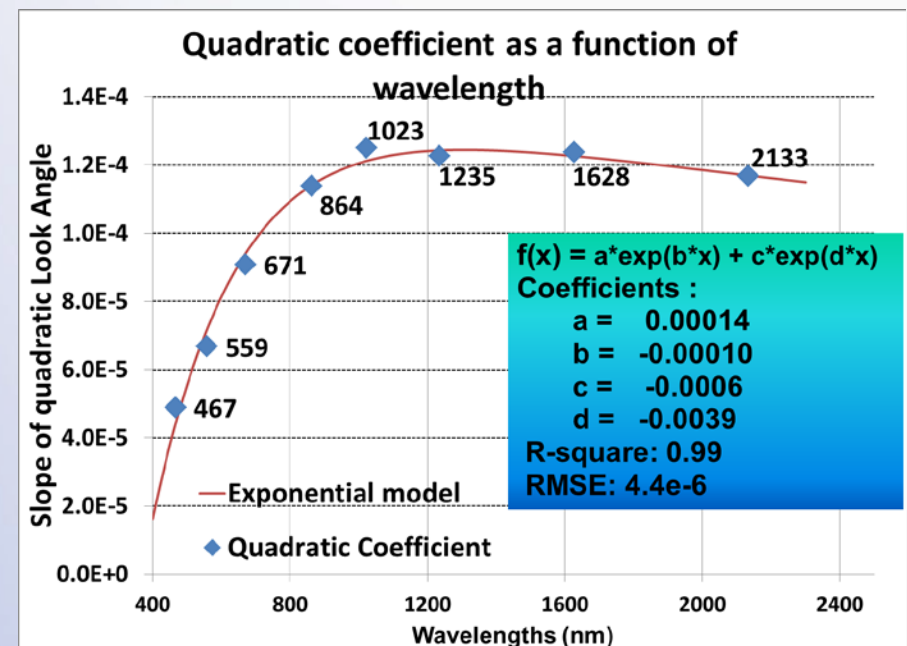
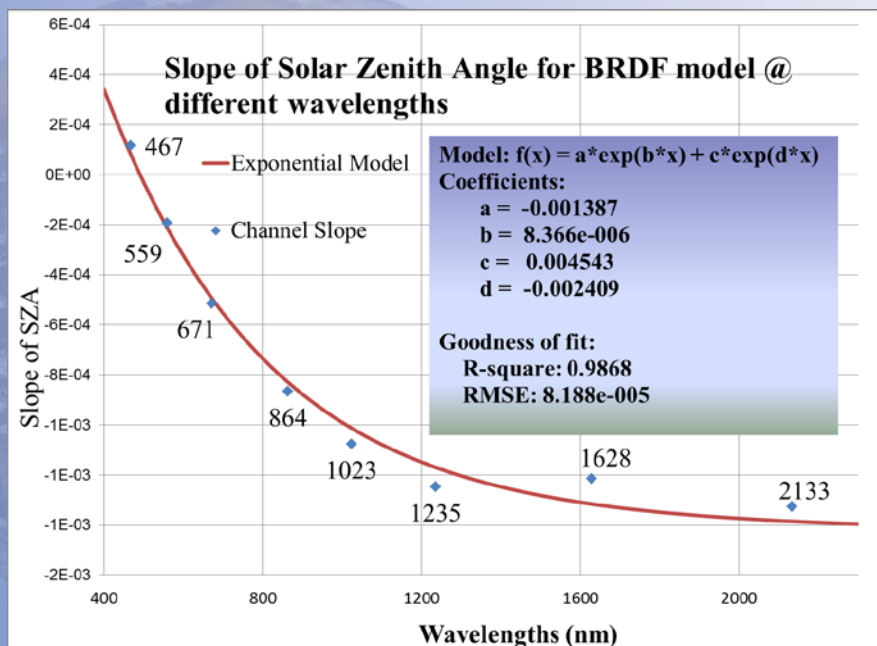
Development of semi-empirical model: Solar Zenith Angle (nadir observations)

- MODIS observations for 10 years used to develop a linear BRDF model to predict the TOA reflectance as a function of solar zenith angle.
- Example shown for red band, similar model was generated for 6 bands.
- The resulting slopes were plotted as a function of their center wavelengths.
- Exponential model developed to predict change in BRDF as a function of wavelength.



Development of Empirical BRDF model

- Similar model was developed for atmospherically cleaner spectral channels across the Hyperion wavelengths
- The model coefficients were then plotted as a function of wavelength.
- The two term exponential model was developed to predict the change in BRDF as a function of wavelength, the first order term of view angle was essentially constant.



Including Atmospheric Modeling in Absolute Calibration Model

Procedure

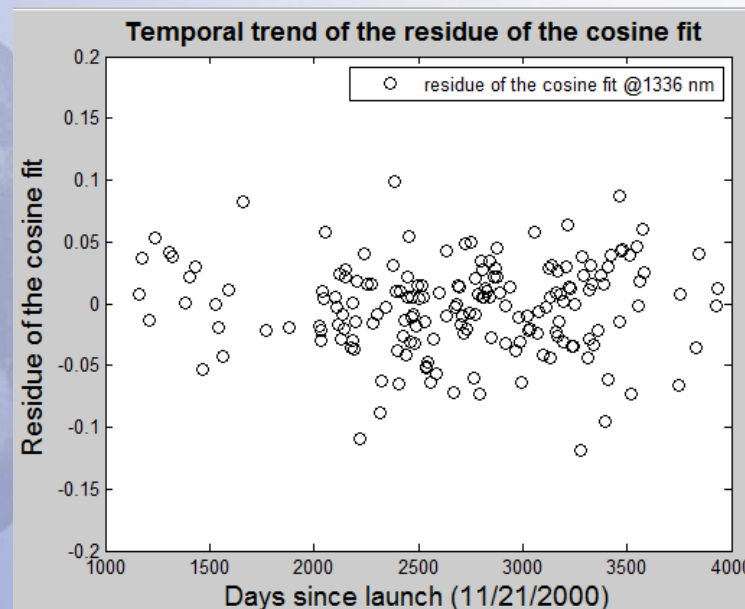
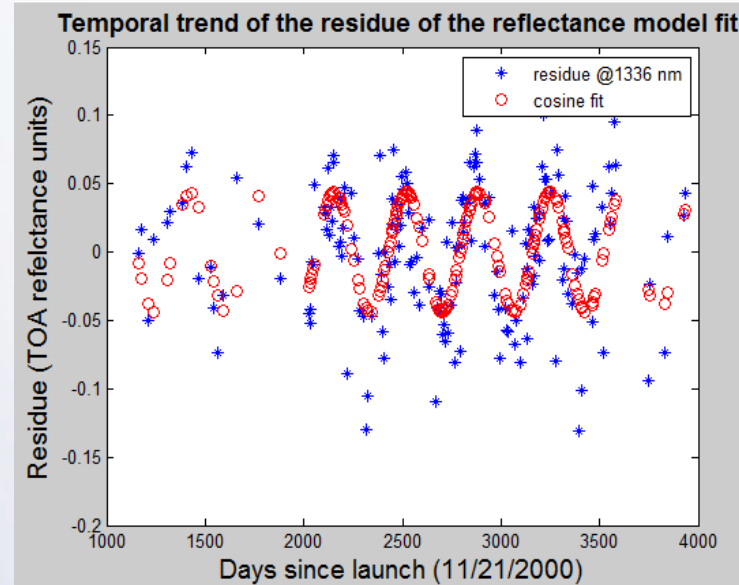
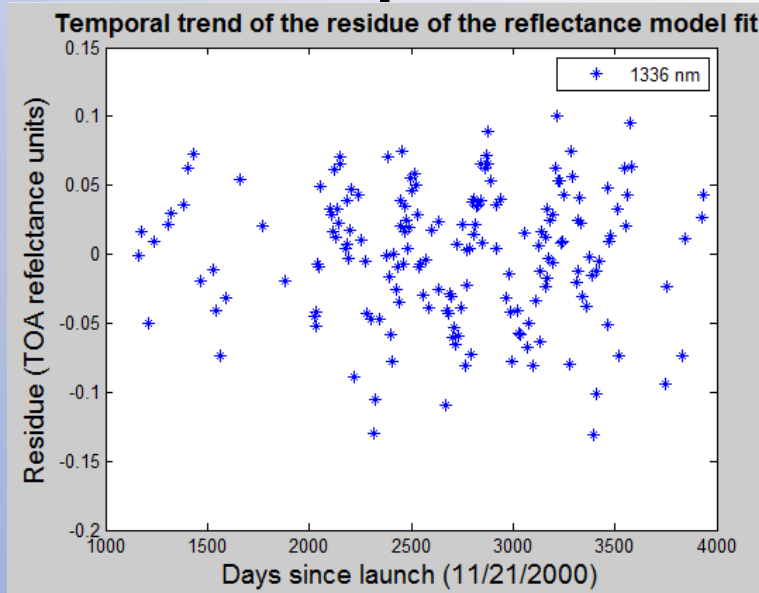
- Each Hyperion channel were modeled using the empirical approach

$$\rho(\theta_{SZ}, \theta_{VZ}, \lambda) = a_{\lambda} + b_{\lambda} * \theta_{SZ} + c_{\lambda} * \theta_{VZ} + d_{\lambda} * \theta_{VZ}^2$$

- Residue of the fit was then calculated for each wavelength.
- A fit of the form $f_A(t) = a_0 + \sum_{n=1}^{\infty} \left(a_n \cos \frac{n\pi t}{T} + b_n \sin \frac{n\pi t}{T} \right)$ was applied to this residue to model the periodic atmospheric cycle in the Hyperion channels where $T=365.2$.
- For simplicity, the first order form with $n=1$ was considered.
- Thus the final absolute calibration model is of the form

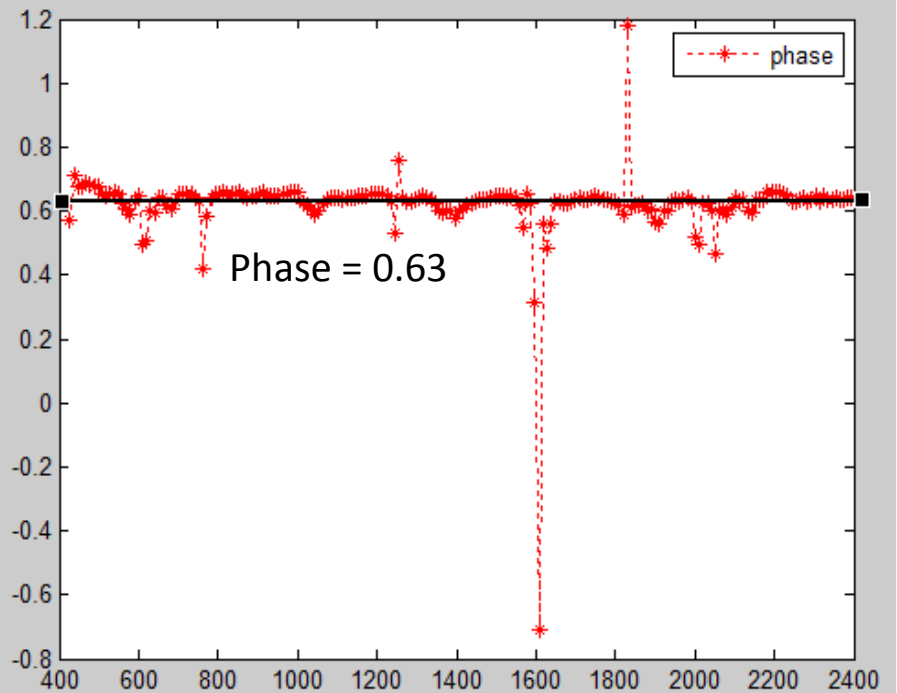
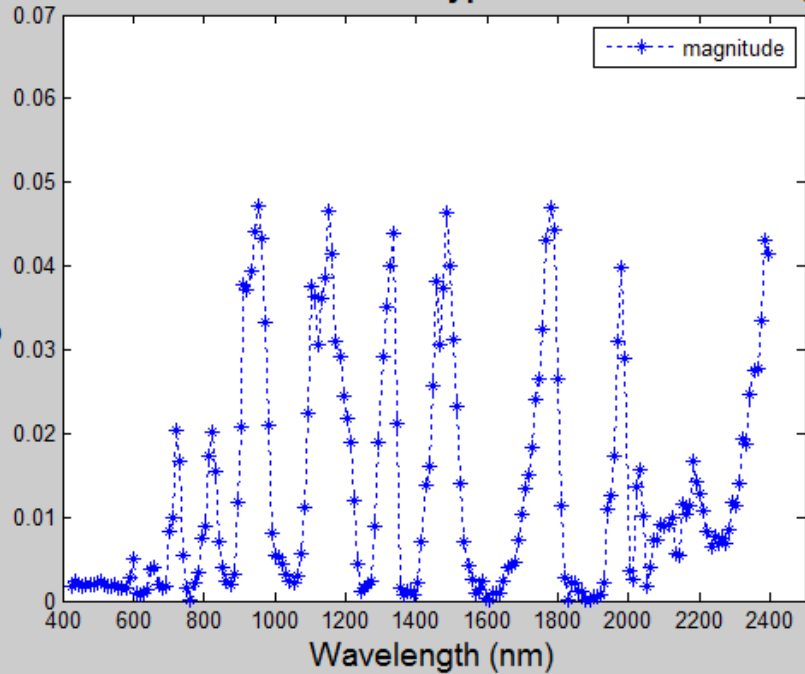
$$\rho_{Libya4}(\lambda, SZA, VZA) = \frac{K(\lambda) * \rho_h(\lambda) * f_A(t)}{[1 - (SZA - 30^\circ) * m_1(\lambda) - VZA(\lambda) * m_2(\lambda) - (VZA)^2 * m_3(\lambda)]}$$

Atmospheric Model Development



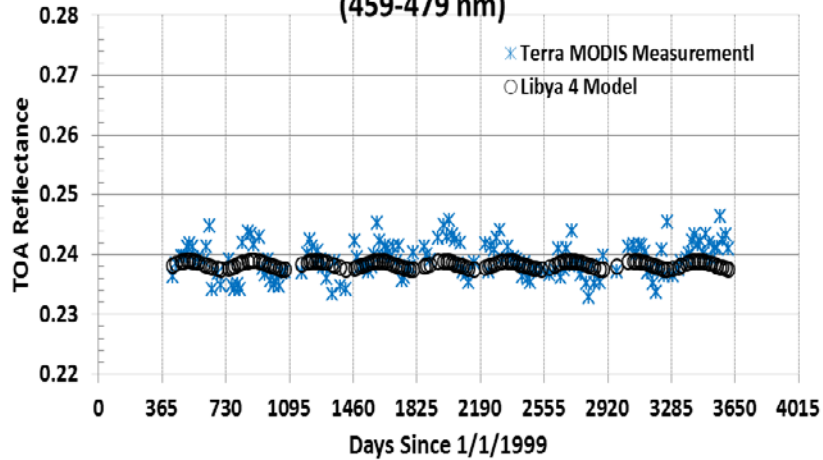
Magnitude and phase spectra of the cosine fit

Manitude of a cosine fit Vs. Hyperion center wavelength

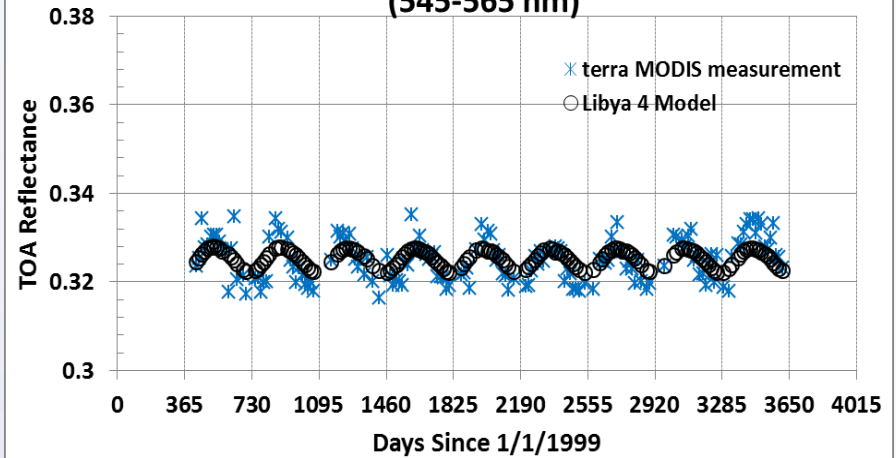


Validation for Terra MODIS (blue & green bands)

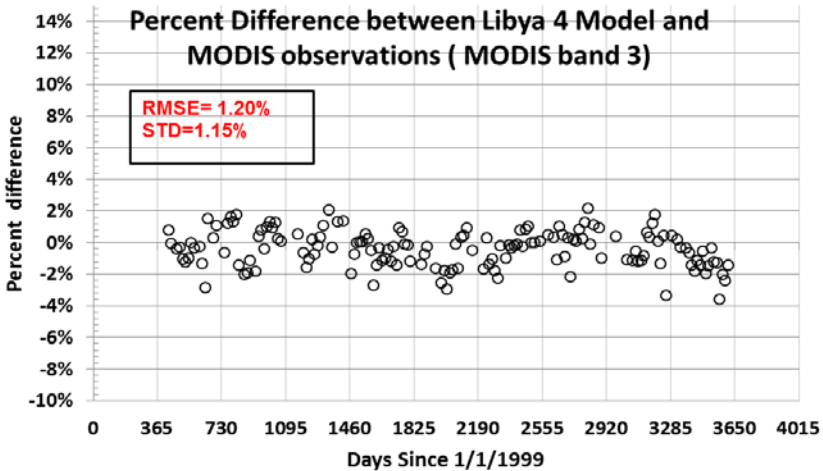
Temporal Trend of MODIS over Libya 4 - Band 3
(459-479 nm)



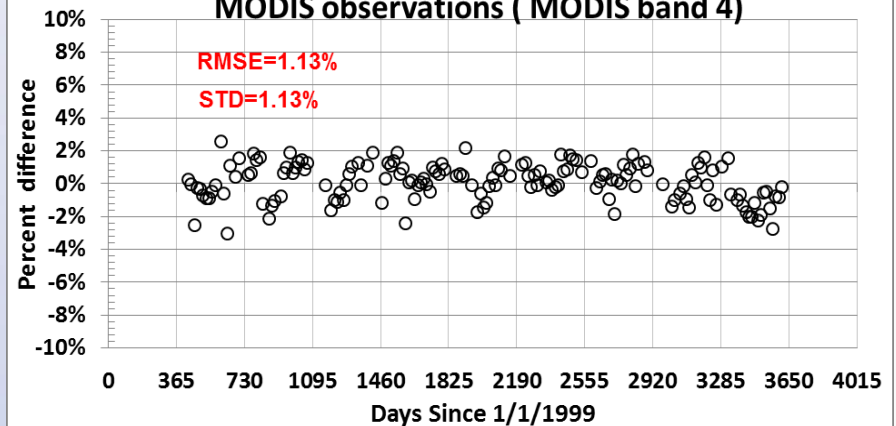
Temporal Trend of MODIS over Libya 4 - Band 4
(545-565 nm)



Percent Difference between Libya 4 Model and
MODIS observations (MODIS band 3)

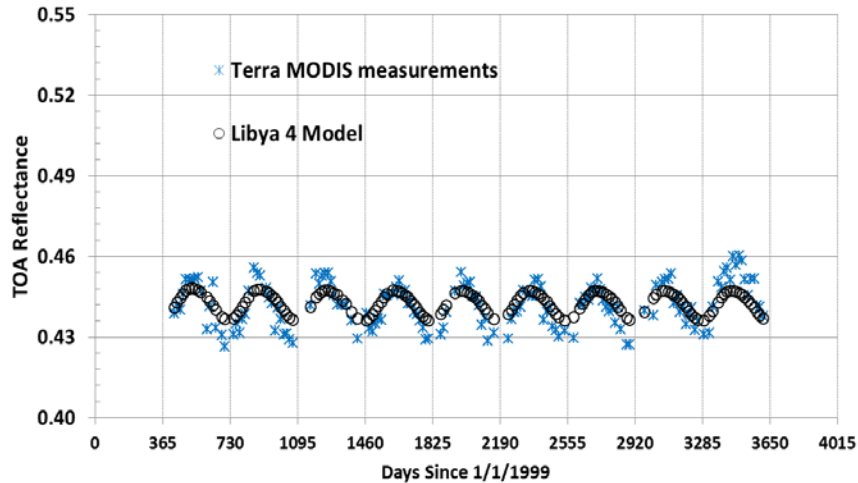


Percent Difference between Libya 4 Model and
MODIS observations (MODIS band 4)

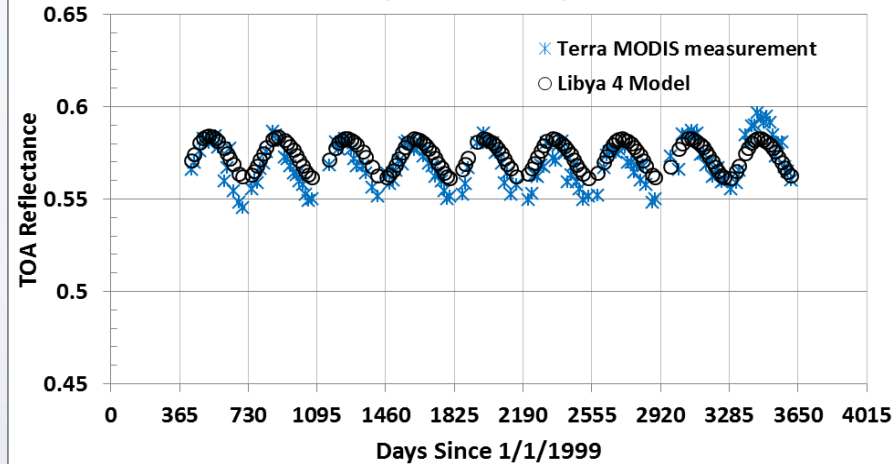


Validation for Terra MODIS (Red & VNIR bands)

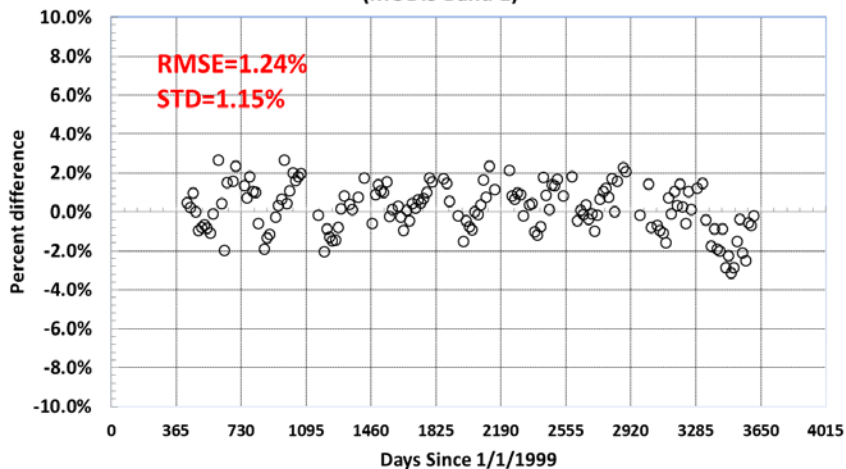
Temporal Trend of MODIS over Libya 4 - Band 1 (620-670 nm)



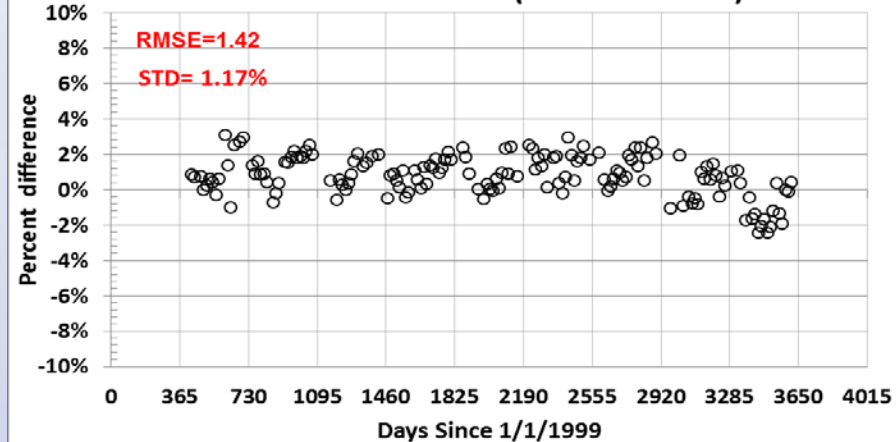
Temporal Trend of MODIS over Libya 4 - Band 2 (841-876 nm)



Percent Difference between Libya 4 Model and MODIS measurements (MODIS Band 1)

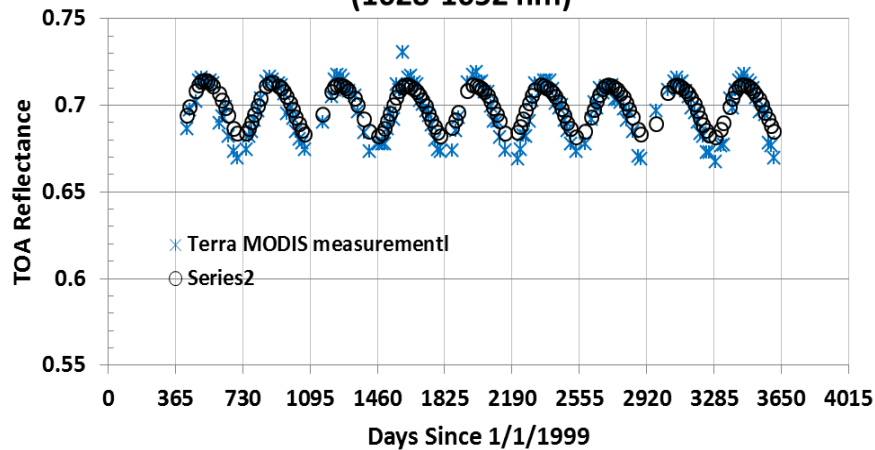


Percent Difference between Libya 4 Model and MODIS observations (MODIS band 2)

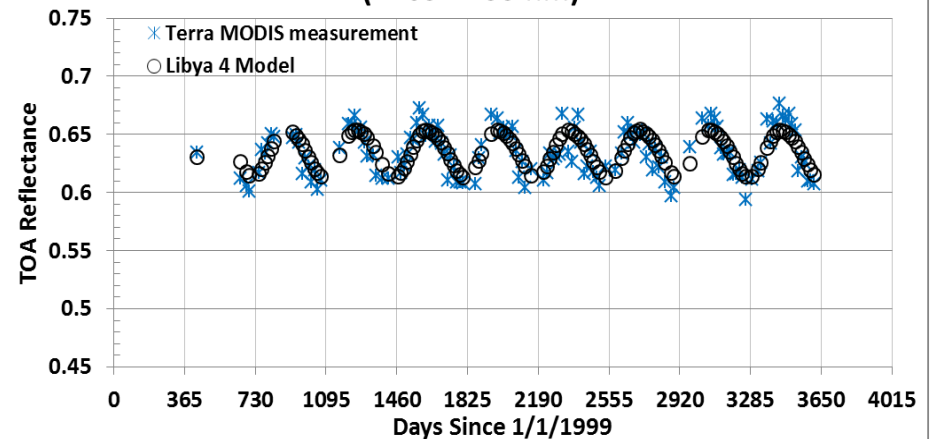


Validation for Terra MODIS (SWIR-1 & SWIR-2 bands)

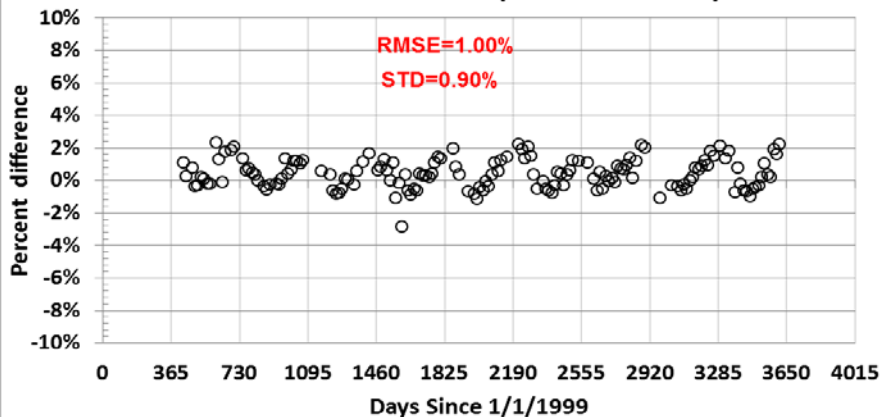
Temporal Trend of MODIS over Libya 4 - Band 6 (1628-1652 nm)



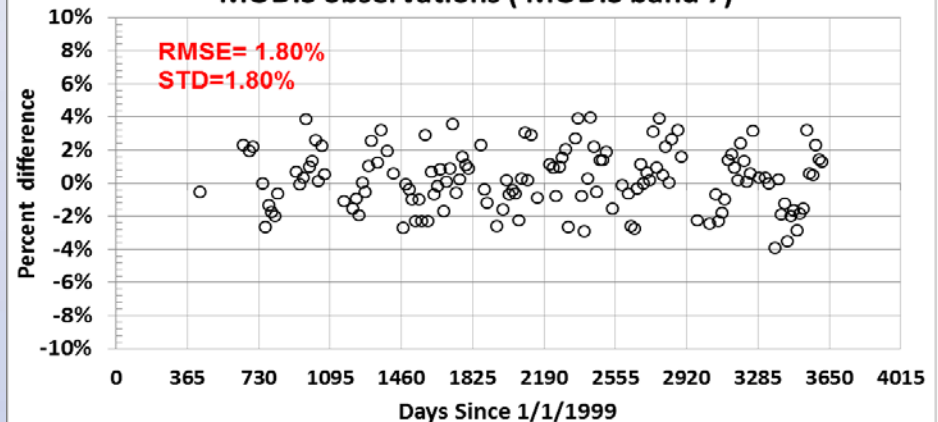
Temporal Trend of MODIS over Libya 4 - Band 7 (2105-2155 nm)



Percent Difference between Libya 4 Model and MODIS observations (MODIS band 6)

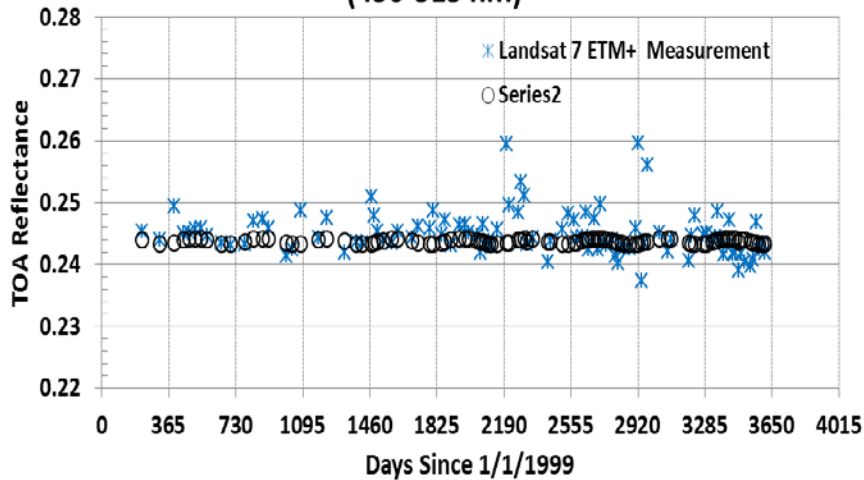


Percent Difference between Libya 4 Model and MODIS observations (MODIS band 7)

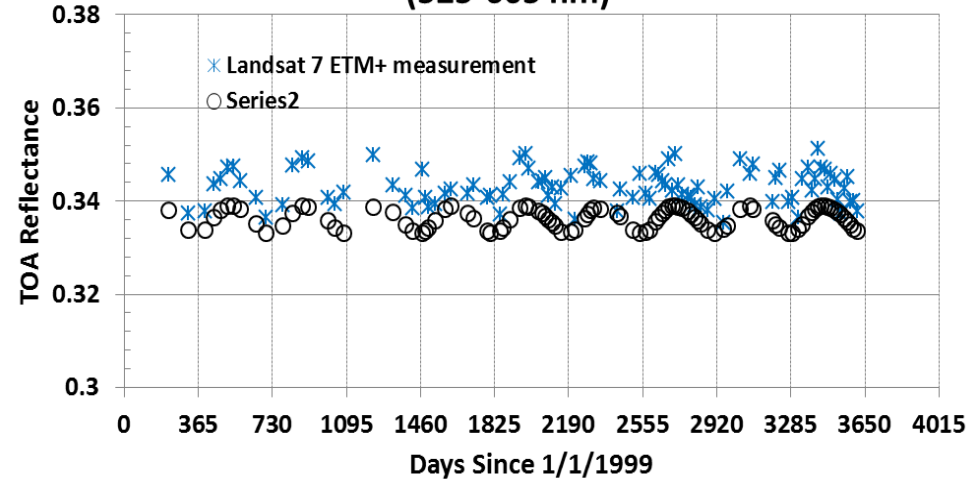


Validation for Landsat ETM+ (Blue & Green bands)

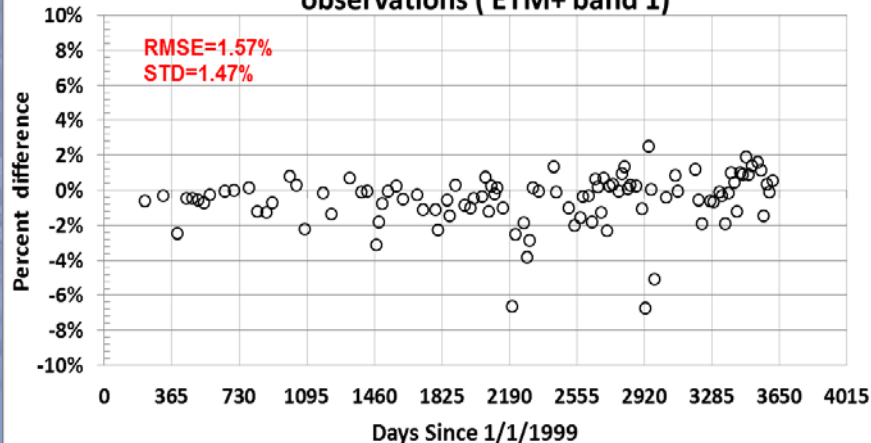
Temporal Trend of ETM+ over Libya 4 - Band 1
(450-515 nm)



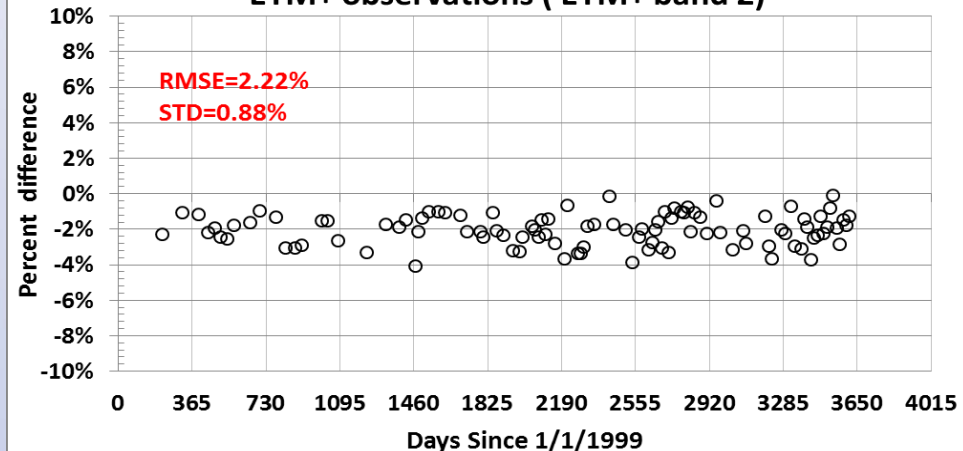
Temporal Trend of ETM+ over Libya 4 - Band 2
(525-605 nm)



Percent Difference between Libya 4 Model and ETM+ observations (ETM+ band 1)

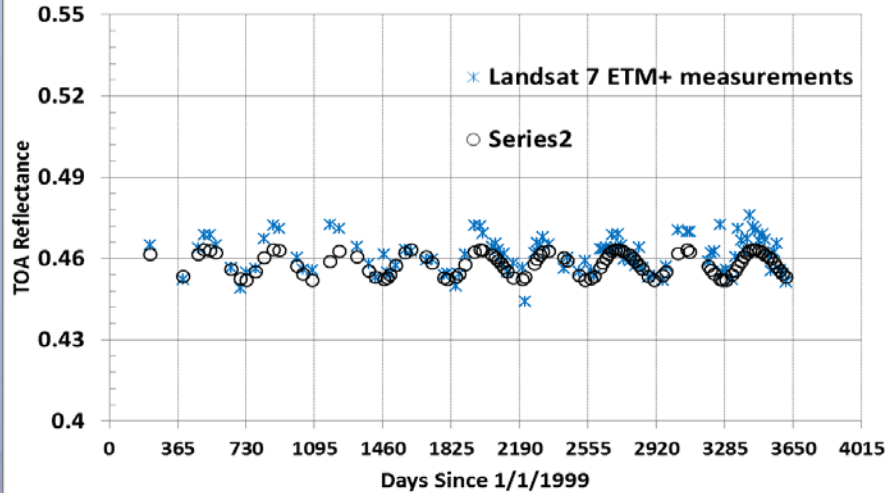


Percent Difference between Libya 4 Model and ETM+ observations (ETM+ band 2)

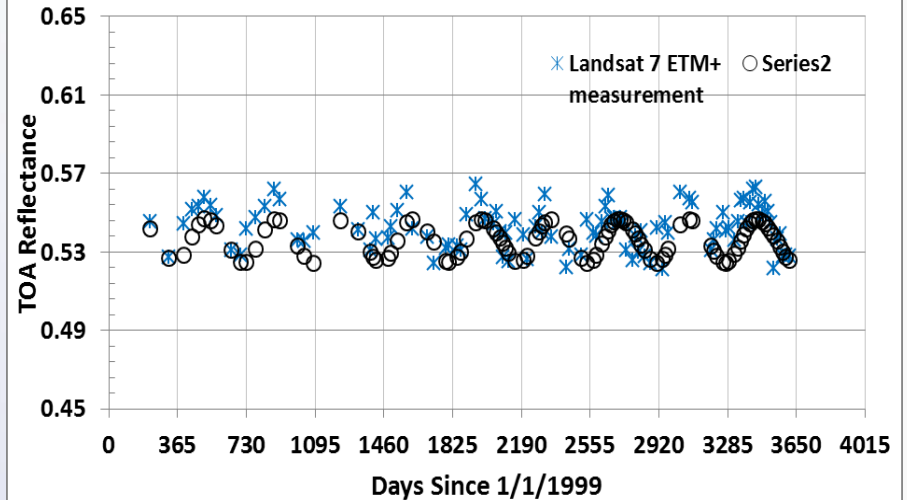


Validation for Landsat ETM+ (Red & VNIR bands)

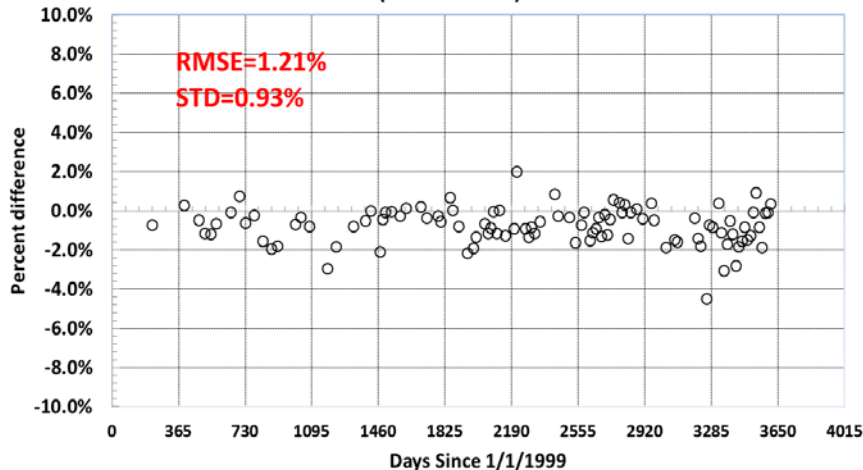
Temporal Trend of ETM+ over Libya 4 - Band 3
(630-690 nm)



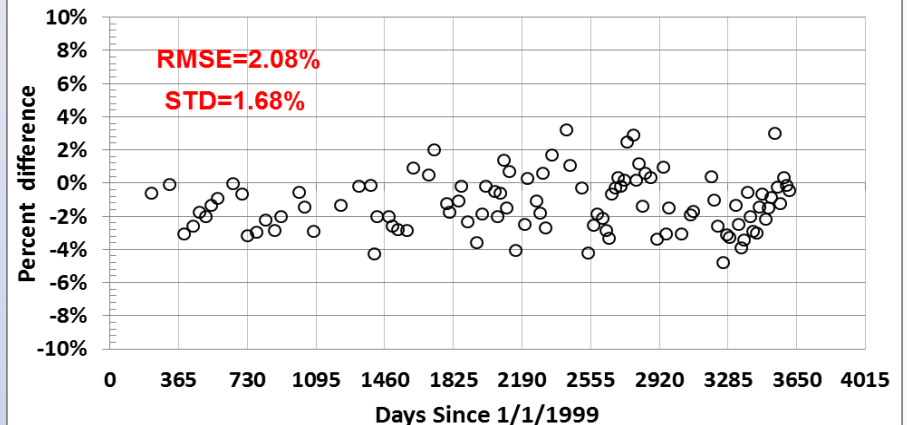
Temporal Trend of ETM+ over Libya 4 - Band 4
(750-900 nm)



Percent Difference between Libya 4 Model and ETM+ measurements
(ETM+ Band 3)

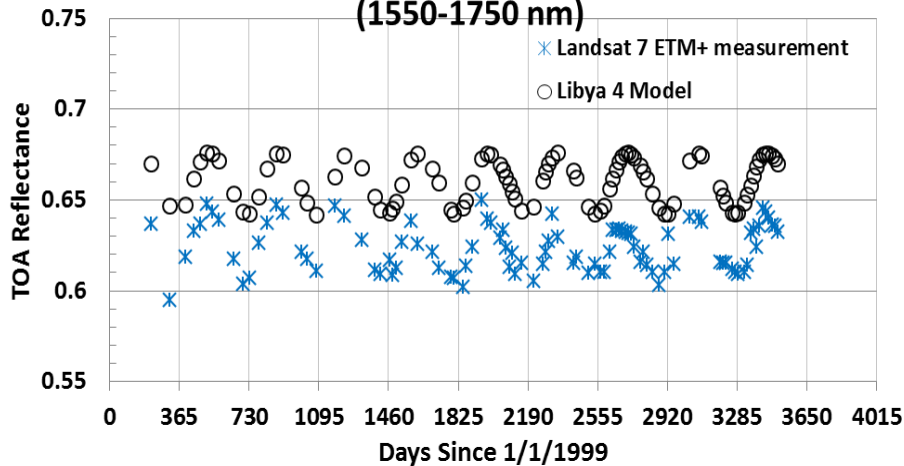


Percent Difference between Libya 4 Model and ETM+ observations (ETM+ band 4)

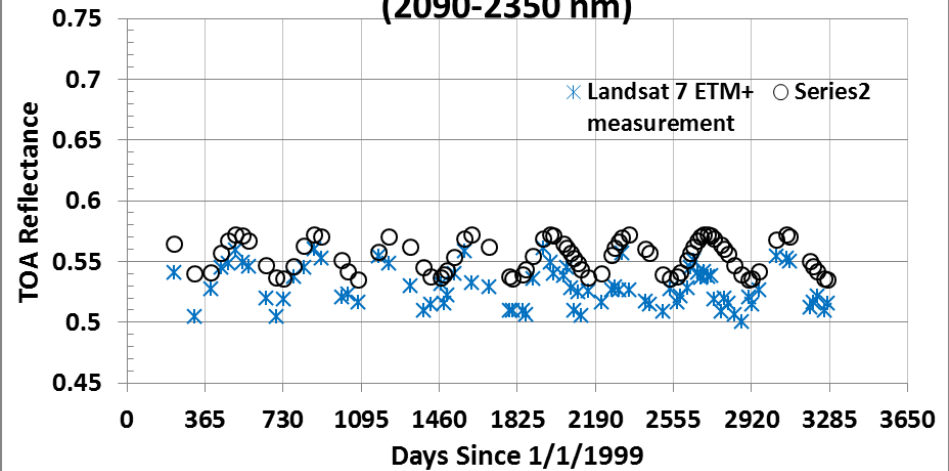


Validation for Landsat ETM+ (SWIR-1 & SWIR-2)

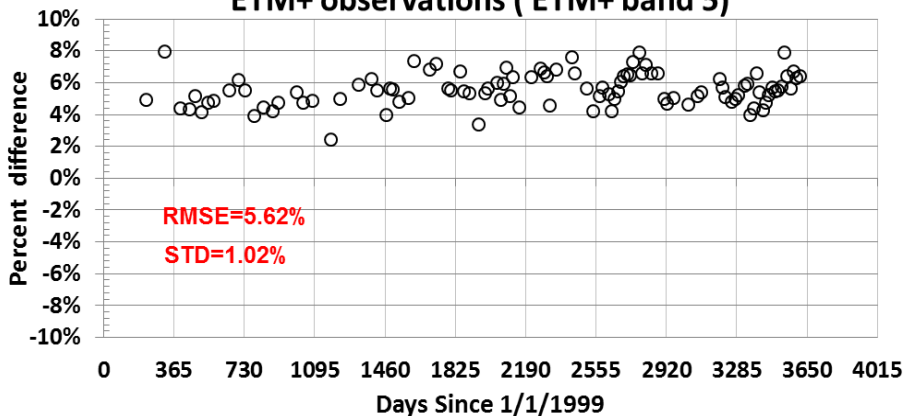
Temporal Trend of ETM+ over Libya 4 - Band 5 (1550-1750 nm)



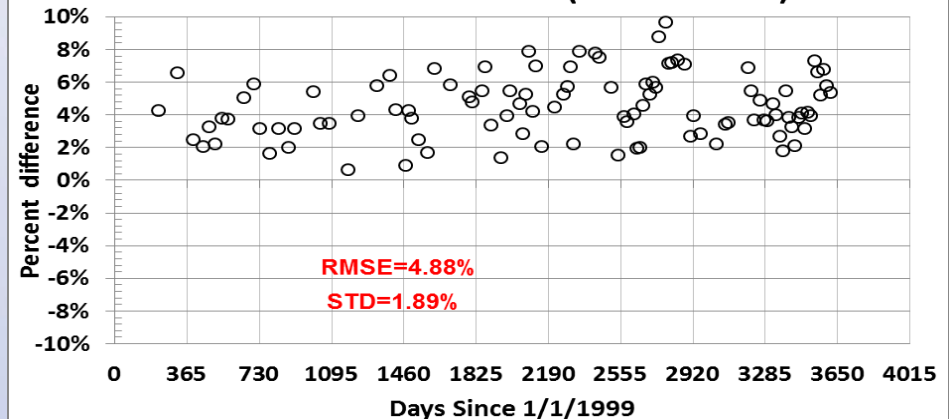
Temporal Trend of ETM+ over Libya 4 - Band 7 (2090-2350 nm)



Percent Difference between Libya 4 Model and ETM+ observations (ETM+ band 5)



Percent Difference between Libya 4 Model and ETM+ observations (ETM+ band 7)



Results

Before atmospheric modeling

MODIS Bands	ETM+ Bands	Root Mean Squared Error (RMSE)		STD of residues	
		MODIS	ETM+	MODIS	ETM+
3 (459-479 nm)	1 (450-515 nm)	1.32%	1.65%	1.26%	1.54%
4(545-565 nm)	2(525-605 nm)	1.24%	2.27%	1.24%	0.94%
1 (620-670 nm)	3 (630-690 nm)	1.39%	1.28%	1.28%	1.02%
2 (841-876 nm)	4 (750-900 nm)	1.61%	2.18%	1.41%	1.79%
6 (1628-1652 nm)	5 (1550-1750 nm)	1.04%	5.70%	0.95%	1.25%
7 (2105-2155 nm)	7 (2090-2350 nm)	2.14%	4.99%	2.15%	2.24%

After atmospheric modeling

MODIS Bands	ETM+ Bands	Root Mean Squared Error (RMSE)		STD of residues	
		MODIS	ETM+	MODIS	ETM+
3 (459-479 nm)	1 (450-515 nm)	1.20%	1.57%	1.15%	1.47%
4(545-565 nm)	2(525-605 nm)	1.13%	2.22%	1.13%	0.88%
1 (620-670 nm)	3 (630-690 nm)	1.24%	1.21%	1.15%	0.93%
2 (841-876 nm)	4 (750-900 nm)	1.42%	2.09%	1.17%	1.68%
6 (1628-1652 nm)	5 (1550-1750 nm)	1.00%	5.62%	0.90%	1.02%
7 (2105-2155 nm)	7 (2090-2350 nm)	1.81%	4.88%	1.80%	1.89%

Accuracy, Precision and SI Traceability

- Accuracy
 - Overall accuracy of the model is based on accuracy of Terra MODIS and Hyperion
 - Terra MODIS accuracy = 3% reflectance-based with on-board solar diffuser
 - Hyperion accuracy = 5% radiance-based prelaunch absolute; recent estimates at SDSU suggest 5% relative, too.
 - Overall model accuracy approximately orthogonal sum = 5.8%
 - Consistent with results
- Precision
 - Experimental results indicate 2% or better thus far
- SI Traceability
 - Based on traceability of the absolute radiometer and spectrometer
 - Both NIST traceable at time of launch
 - Post-launch traceability more difficult to determine
 - Significant limitation of this approach

Discussion/Conclusions/Future Work

- Simple empirical models based on observations from space can trend sensors with precision of 2% or better.
 - Results suggest PICS stability of better than 1%
 - Limitations based on TOA-based surface characterization and limited atmospheric model.
- Absolute calibration using space-based radiometers clearly dependent on their performance
 - Roughly 5.8% for this approach
 - CLARREO and TRUTHS please!
- Model development currently limited
 - Need broader range of viewing angles
 - Consideration of PM sensors
 - Better atmospheric modeling possible
- Source-based model
 - Potential to address accuracy limitation
 - Dependent on surface model and atmospheric model improvement
 - Following speaker will elaborate further!